Growth Hormone-Dependent Pathogenesis of Human Hepatic Steatosis in a Novel Mouse Model Bearing a Human Hepatocyte-Repopulated Liver

Chise Tateno, Miho Kataoka, Rie Utoh, Asato Tachibana, Toshiyuki Itamoto, Toshimasa Asahara, Fuyuki Miya, Tatsuhiko Tsunoda, and Katsutoshi Yoshizato

Yoshizato Project (C.T., M.K., R.U., A.T., K.Y.), Hiroshima Prefectural Institute of Industrial Science and Technology, Cooperative Link of Unique Science and Technology for Economy Revitalization (CLUSTER), and PhoenixBio, Co. Ltd. (C.T., A.T., K.Y.), Higashihirosima, Hiroshima 739-0046, Japan; Hiroshima University Liver Project Research Center (C.T., T.A., K.Y.) and Division of Frontier Medical Science (T.I., T.A.), Department of Surgery, and Hiroshima University 21st Century COE Program for Advanced Radiation Casualty Medicine, Programs for Biomedical Research, Graduate School of Biomedical Sciences, Hiroshima University, Hiroshima, Hiroshima 734-8551, Japan; Laboratory for Medical Informatics (F.M., T.T.), Center for Genomic Medicine, RIKEN, Yokohama, Kanagawa 230-0045, Japan; Developmental Biology Laboratory and Hiroshima University 21st Century COE Program for Advanced Radiation Casualty Medicine (K.Y.), Department of Biological Science, Graduate School of Science, Hiroshima University, Higashihiroshima, Hiroshima 739-8526, Japan; and Departments of Hepatology and Liver Research Center (K.Y.), Graduate School of Medicine, Osaka City University, Osaka 545-8586, Japan

Clinical studies have shown a close association between nonalcoholic fatty liver disease and adult-onset GH deficiency, but the relevant molecular mechanisms are still unclear. No mouse model has been suitable to study the etiological relationship of human nonalcoholic fatty liver disease and human adult-onset GH deficiency under conditions similar to the human liver *in vivo*. We generated human (h-)hepatocyte chimeric mice with livers that were predominantly repopulated with h-hepatocytes in a h-GH-deficient state. The chimeric mouse liver was mostly repopulated with h-hepatocytes about 50 d after transplantation and spontaneously became fatty in the h-hepatocyte regions after about 70 d. Infusion of the chimeric mouse with h-GH drastically decreased steatosis, showing the direct cause of h-GH deficiency in the generation of hepatic steatosis. Using microarray profiles aided by real-time quantitative RT-PCR, comparison between h-hepatocytes from h-GH-untreated and -treated mice identified 14 GH-up-regulated and four GH-down-regulated genes, including *IGF-I, SOCS2, NNMT, IGFLS, P4AH1, SLC16A1, SRD5A1, FADS1*, and *AKR1B10*, respectively. These GH-up- and -down-regulated genes were expressed in the chimeric mouse liver at lower and higher levels than in human livers, respectively. Treatment of the chimeric mice with h-GH ameliorated their altered expression. h-Hepatocytes were separated from chimeric mouse livers for testing *in vitro* effects of h-GH or h-IGF-I on gene expression, and results showed that GH directly regulated the expression of *IGF-I, SOCS2, NNMT, IGFALS, P4AH1, FADS1*, and *AKR1B10*. In conclusion, the chimeric mouse is a novel h-GH-deficient animal model for studying *in vivo* h-GH-dependent human liver dysfunctions. (*Endocrinology* 152: 0000–0000, 2011)

To study pathophysiological characteristics of the human liver, we previously generated a humanized (chimeric) mouse whose liver was almost completely repopulated with human (h-)hepatocytes by transplanting h-hepatocytes into immunodeficient and liver-damaged mice, which had been obtained by mating an albumin enhancer/promoter-driven

Abbreviations: AGHD, Adult-onset GH deficiency; Alb, albumin; CK, cytokeratin; GO, gene ontology; h-, human; m-, mouse; 9MM, 9-month-old male; NAFLD, nonalcoholic fatty liver disease; NASH, nonalcoholic steatohepatitis; ORO, Oil Red O; qRT-PCR, quantitative RT-PCR; RI, replacement index; SCID, severe combined immunodeficient; uPA, urokinase-type plasminogen-activator; 25YF, 25-yr-old female; 61YF, 61-yr-old female; 28YM, 28-yr-old male; 57YM, 57-yr-old male.

urokinase-type plasminogen-activator (uPA) transgenic mouse with a severe combined immunodeficient (SCID) mouse (uPA/SCID mouse) (1–3). The replacement index (RI), the occupancy ratio of h-hepatocytes to the total [h- and mouse (m-)] hepatocytes in the chimeric mouse liver, indicated the degree of replacement with h-hepatocytes. The RI in the mice was as high as 96% (1). h-Hepatocytes therein expressed mRNA for drug-metabolizing enzymes and transporters as in donor livers (1, 4, 5). However, we noticed that the mice spontaneously developed hepatic steatosis as the time after transplantation was prolonged. The h-hepatocytes of a chimeric mouse are in a GH-deficient state (6) primarily because human cells do not react with rodent GH (7), thus suggesting that the observed lipid accumulation in h-hepatocytes was caused by a lack of available h-GH in chimeric mice.

A concern is increasing about nonalcoholic fatty liver disease (NAFLD) as a significant complication of obesity and as a hepatic manifestation of the metabolic syndrome (8). There are striking similarities between obesity and untreated adult-onset GH deficiency (AGHD), indicating that homeostatic imbalance of GH is an etiological factor of obesity (9). NAFLD is related to hypopituitary and hypothalamic dysfunction (10–12). AGHD is featured as decrease in body mass, increase in visceral adiposity, and abnormal lipid profile (13), which are associated with hepatic steatosis (11, 13, 14). One study showed that reduction in GH concentration was a predictor of NAFLD in adult males (15) and another that GH administration drastically improved the fatty liver of AGHD patients (13, 14). A suitable GH-dependent lipogenetic animal model is currently absent, in which we can investigate the *in vivo* effects of h-GH on h-hepatocytes at the cellular and molecular levels.

In this study, we first tested the hypothesis that h-hepatocytes in chimeric mouse liver develop steatosis due to the lack of circulating h-GH. In fact, hepatic steatosis was induced in the mouse liver but not when the chimeric mice were treated with h-GH. We then compared gene expression profiles between h-GH-treated and -untreated chimeric mouse h-hepatocytes to identify h-GH-regulated lipogenesis genes. Furthermore, we examined whether h-GH directly regulates the expression of lipogenesis-related genes or of h-IGF-I levels using cultured chimeric mouse h-hepatocytes. As a whole, the chimeric mouse was proved to be a suitable animal model for studying the etiological relationship among AGHD, GH, and NAFLD in GH-related aspects of metabolic syndrome.

Materials and Methods

We performed studies under the ethical approval of the Hiroshima Prefectural Institute of Industrial Science and Technology

Ethics Board and the Ethics Committee at the Hiroshima University Hospital.

Preparation of h-hepatocytes

Livers were obtained from four donors [a 28-yr-old male (28YM) and a 57-yr-old male (57YM) and a 25-yr-old female (25YF) and a 61-yr-old female (61YF)] after receiving informed consent before surgery, according to the 1975 Declaration of Helsinki. h-Hepatocytes were isolated from the liver tissues as previously reported (1). Real-time quantitative RT-PCR (qRT-PCR) was performed on these human livers and/or on h-hepatocytes isolated from h-liver tissues (Table 1).

Donor cells for chimeric mice were h-hepatocytes from a Caucasian 9-month-old male (9MM) infant and an African-American 6-yr-old girl (6YF) purchased from In Vitro Technologies (Baltimore, MD) and BD Biosciences Discovery Labware (San Jose, CA), respectively.

Animals, transplantation of h-hepatocytes, and treatment of chimeric mice with h-GH

Production of uPA/SCID mice (1) and examination of their zygosity in uPA transgenes (16) were performed as previously reported. Homozygotic mice (20–30 d old) were used as hosts for all transplantation experiments. The 9MM and 6YF hepatocytes (hepatocytes$_{9MM}$ and hepatocytes$_{6YF}$, respectively), 7.5–10.0 × 10^5 cells per animal, were transplanted into six uPA/SCID mice (Table 2) for microarray and real-time qRT-PCR analysis and into 41 mice [36 mice for steatosis analysis (Fig. 1C) and five mice for steatosis analysis under h-GH treatment (Fig. 2E)], as previously described (1). Chimeric mice were killed 48–118 d after transplantation.

Three chimeric mice with hepatocytes$_{9MM}$ [nos. 4–6 (Table 2)], three chimeric mice with hepatocytes$_{6YF}$ [nos. 4–6 (Table 2)], one chimeric mouse$_{9MM}$ (not included in Table 2), and one chimeric mouse$_{6YF}$ (not included in Table 2) were continuously infused with 2.5 mg/kg·d h-GH (Wako, Osaka, Japan) through an sc-implanted Alzet micro-osmotic pump (Alza Corp., Palo Alto, CA) for 2 wk before killing (6, 17). Blood h-albumin (Alb) and serum h-IGF-I in the mice were quantified as previously reported (6).

Immunohistochemistry, lipid staining, and grading of steatosis in h-hepatocytes of chimeric mouse liver

Formalin-fixed paraffin sections from the left lateral lobe of six chimeric mice$_{6YF}$ were stained with mouse anti-h-cytokeratin (CK) 18 monoclonal antibodies (clone CD10; Dako Cytomation, Glostrup, Denmark) that did not react m-hepatocytes as

TABLE 1. Human liver tissues used in real-time qRT-PCR

Objectives	Age (yr)	Sex	RT-PCR
25YF	25	F	Cell and tissue
28YM	28	M	Cell and tissue
57YM	57	M	Cell
61YF	61	F	Cell and tissue

F, Female; M, male.

TABLE 2. Chimeric mice used in microarray analysis and real-time qRT-PCR

Donors	Animal number (sex)	Treatment with h-GH[a]	Days after transplantation	h-Alb in blood (mg/ml)	h-IGF-I in sera (ng/ml)	RI$_{Alb}$ (%)[b] or RI$_{immuno}$ (%)[c]	Microarray or RT-PCR
9MM	1 (F)	−	72	16.1	ND	>95[b]	Cell
	2 (F)	−	75	10.4	ND	>95[b]	
	3 (F)	−	101	6.0	ND	80[b]	
	4 (M)	+	75	8.1	ND	95[b]	
	5 (F)	+	75	6.2	ND	80[b]	
	6 (F)	+	75	5.9	ND	80[b]	
6YF	1 (F)	−	97	3.5	<9.4	75.1[c]	Tissue
	2 (F)	−	90	6.5	<9.4	78.1[c]	
	3 (F)	−	111	5.2	<9.4	70.2[c]	
	4 (M)	+	84	5.3	69.6	85.3[c]	
	5 (F)	+	84	3.7	64.8	70.3[c]	
	6 (F)	+	84	5.9	83.0	81.5[c]	

F, Female; M, male; ND, not determined.

[a] −, untreated with h-GH; +, treated with hGH.

[b] RI calculated by the blood h-Alb levels using the formula of the correlation curve $y = 0.0006x^2 + 0.0281x - 0.0042$ ($r^2 = 0.60$) in which x and y represent RI and blood h-Alb level, respectively.

[c] RI determined by immunohistological staining of liver sections.

previously described (18). The area occupied by h-CK18-positive (h-CK18$^+$) hepatocytes was identified to calculate RI (1).

Frozen sections were prepared from the livers of five h-GH-treated and 36 chimeric h-GH-untreated mice$_{6YF}$ and stained with Oil Red O (ORO). When necessary, serial sections were stained with anti-h-CK8/18 antibodies (MP Biomedicals, Aurora, OH) that did not react with m-hepatocytes as previously described (19). Steatosis grading of h-hepatocytes was performed on ORO-stained chimeric mouse liver sections as follows: grade 0, no lipid droplets; grade 1, appearance of small lipid droplets; grade 2, small and middle-sized lipid droplets; grade 3, small to large droplets (Fig. 1B).

Isolation of h-hepatocytes from chimeric mouse livers for gene expression profiles

Livers were isolated 72–101 d after transplantation from h-GH-untreated control chimeric mice$_{9MM}$ [nos. 1–3 (Table 2)] and h-GH-treated chimeric mice$_{9MM}$ [nos. 4–6 (Table 2)]. These livers were disaggregated by two-step collagenase perfusion as previously described (20), except perfusion was for 20 min and centrifugation was three times 2 min at 50 × g. Pelleted hepatocytes (h-hepatocytes$_{chimeric mouse}$) were treated with RLT buffer solution in an RNeasy Mini kit (QIAGEN K.K., Tokyo, Japan) and stored in a deep freezer until RNA isolation for microarray and real-time qRT-PCR.

Purity of h-hepatocytes$_{chimeric mouse}$

We previously established the correlation curve for chimeric mice$_{9MM}$ between the blood h-Alb concentration and RI$_{immuno}$, which is determined immunohistologically from liver tissue sections (1). The correlation curve predicted that chimeric mice$_{9MM}$ for microarray and real-time qRT-PCR examinations had a RI$_{Alb}$ higher than 80% (Table 2). Apparently, this RI was a lower estimation of the real h-hepatocyte purity in hepatocyte preparations because m-hepatocytes were often lost during collagenase digestion due to fragility against the enzyme. Thus, the correct h-hepatocyte purity in the hepatocytes$_{chimeric mouse/9MM}$ (hepatocytes isolated from chimeric mouse liver bearing h-hepatocytes$_{9MM}$) was determined as follows. Among chimeric

mice$_{6YF}$, we selected 10 mice whose RI$_{Alb}$ at the time of death was similar to that of the chimeric mice$_{9MM}$ and isolated h-hepatocytes$_{chimeric mouse}$ from them. They were incubated with K8216 antibodies that react with the cell surface of h- but not m-hepatocytes (21) and then with secondary antibody, followed by fluorescence-activated cell sorting analysis to determine the percentage of h-hepatocytes in the hepatocytes$_{chimeric mouse}$. The h-hepatocyte purity was 90.8 ± 6.4% (n = 10). The presence of m-hepatocytes in hepatocytes$_{chimeric mouse}$ at less than 10% did not affect microarray assays as described in *Results*.

Microarray analysis

RNAs were extracted using TRIzol reagent (Invitrogen, Carlsbad, CA) from h-hepatocytes and h-liver tissues isolated from h-GH-untreated and -treated chimeric mice and were used for microarray analysis at the hepatocyte and liver tissue levels, respectively (Table 2). The array profiles were compared between h-GH-treated and -untreated samples, and statistical significance tests were performed. We deposited our array data to NCBI GEO (Gene Expression Omnibus, http://www.ncbi.nlm.nih.gov/geo/query/acc.cgi?acc=GSE26224, GEO ID GSE26224).

Microarray at the hepatocyte level

Six chimeric mice$_{9MM}$ [nos. 1–6 (Table 2)] were used in the hepatocyte level microarray assay. Half of the chimeric mice (nos. 1–3) were as h-GH-untreated control animals and the remaining half (nos. 4–6) as h-GH-treated animals by treating with h-GH during the last 2 wk before killing. h-Hepatocytes$_{chimeric mouse}$ were isolated from h-GH-untreated and -treated chimeric mice$_{9MM}$ at 72–101 d and 75 d after transplantation, respectively, for total RNA isolation.

The RNA samples were treated with deoxyribonuclease (QIAGEN K.K.), purified using ribonuclease-free deoxyribonuclease set (QIAGEN K.K.) and RNeasy Mini Kit (QIAGEN K.K.), and applied to an Affymetrix GeneChip Human Genome U133 Plus 2.0 Array (Affymetrix, Santa Clara, CA) that had been spotted with 54,675 human transcripts. Microarray data were normalized using GCOS software version 1.3 (Affymetrix). The
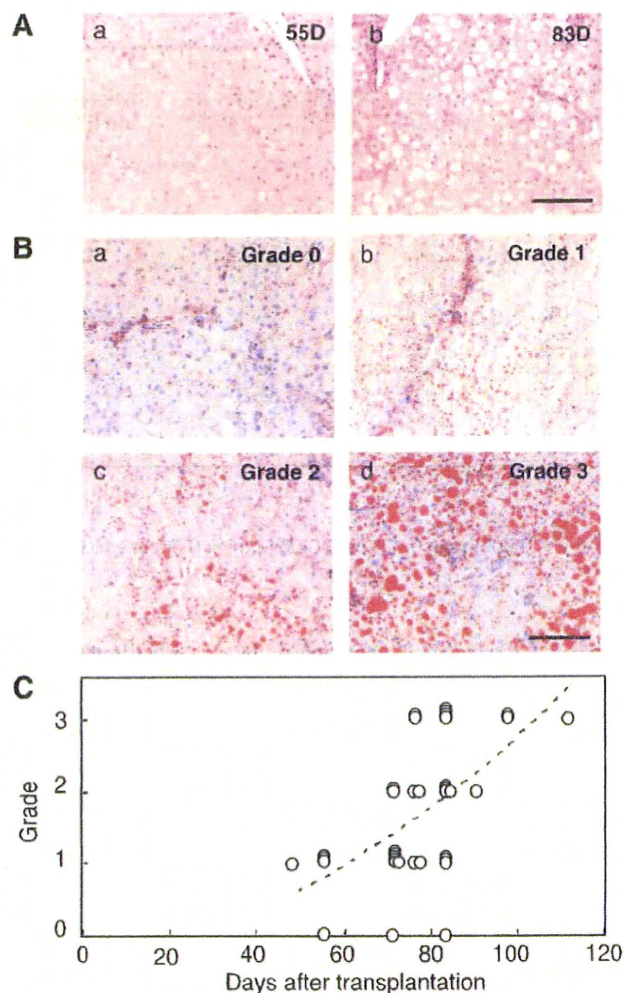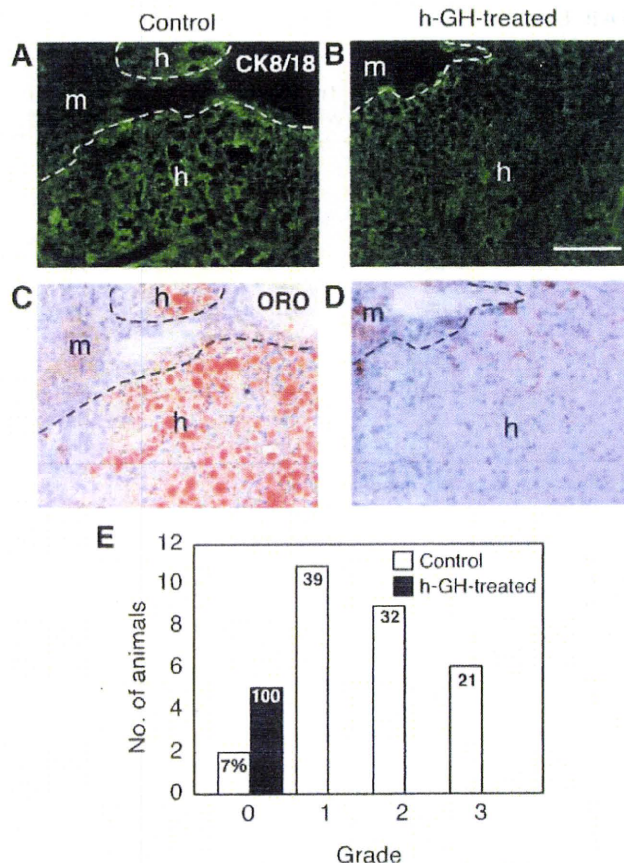
FIG. 1. Lipid accumulation in chimeric mouse h-hepatocytes. Chimeric mice$_{6YF}$ were killed 48–111 d after transplantation for histological examinations by hematoxylin and eosin (A) and ORO liver staining (B). A, h-Hepatocyte regions in the mice killed at 55 d (55D) (a) and 83 d (83D) (b). No visible cytoplasmic vacuolation in the h-hepatocytes at 55 d, but extensive and intensive vacuolation at 83 d. B, Grading of steatosis. Photos of typical staining show various levels of lipid accumulation with nuclei stained *blue*. Lipid accumulation was graded as described in the text: a, grade 0 (55 d); b, grade 1 (77 d); c, grade 2 (83 d); d, grade 3 (97 d). *Bars*, 100 μm. C, Relationship between steatosis grade and duration (days) after transplantation. The steatosis grade increased according to the following relationship: y = 0.0002x^2 + 0.0102x − 0.4416, where x is days after transplantation, and y is steatosis grade. The correlation coefficient was r^2 = 0.3455. The *dashed line* represents the best-fit curve for the above equation.

FIG. 2. Effects of h-GH on liver steatosis. Five chimeric mice$_{6YF}$ were given h-GH in the last 2 wk before being killed 70–90 d after transplantation. Twenty-eight of the mice$_{6YF}$ shown in Fig. 1C were killed at 70–90 d as h-GH-untreated animals. A–D, Histology. A control (6YF, no. 1 in Table 2) (A) and h-GH-treated mouse (6YF no. 4 in Table 2] (B) were killed at 97 and 84 d after h-hepatocyte transplantation, respectively, for h-CK8/18 immunohistochemistry to identify h-hepatocytes. Primary antibodies were visualized with Alexa 594-conjugated anti-m-IgG goat sera (Molecular Probes, Eugene, OR). Serial sections from the control (C) and h-GH-treated mouse (D) were stained with ORO. Small to large droplets are diffusely distributed in h-hepatocytes from control chimeric liver (grade 3) but are absent in h-GH-treated animals (grade 0); m and h indicate regions of m- and h-hepatocytes, respectively. *Dotted lines* show the boundary between the two regions. *Bar*, 100 μm. E, Steatosis graded for 28 controls (*white bars*) and five h-GH-treated chimeric mice (*black bar*). *Arabic numerals* in the *bars* represent the percentage in each case (control or h-GH-treated animals). All h-GH-treated chimeric mice were of grade 0.

obtained mRNA expression profiles were referred to as profiles at the hepatocyte level: profiles of h-GH-untreated (n = 3) and h-GH-treated h-hepatocytes$_{chimeric\ mouse}$ (n = 3).

Microarray analysis at the liver tissue level

Six chimeric mice$_{6YF}$ [nos. 1–6 (Table 2)] were used for the liver tissue-level assay. Half of six chimeric mice$_{6YF}$ (nos. 4–6) were treated with h-GH, and the other half (nos. 1–3) served as controls. Liver tissues consisted of three visually identifiable regions of different colors. White, red, and medium-colored regions between the white and red regions corresponded to those of original diseased m-hepatocytes, uPA gene-deleted m-hepa-

tocytes, and h-hepatocytes, respectively (1). h-Hepatocyte regions were dissected from livers of chimeric mice$_{6YF}$ using a razor blade for RNA extraction. The obtained mRNA expression profiles were referred to as profiles at the liver tissue level.

Determination of gene expression by real-time qRT-PCR

mRNA expression was determined by real time qRT-PCR in human livers and h-GH-untreated and -treated chimeric mouse livers for h-GH-regulated genes selected from microarray analysis and lipogenesis-related genes (Table 3). Sources for extraction of total RNA are shown in Tables 1 and 2. cDNA was

TABLE 3. Primers

Gene	Forward primers (5'–3')	Reverse primers (5'–3')
IGF-I	GCTTCCGGAGCTGTGATCTAA	GCTGACTTGGCAGGCTTG
SOCS2	GCAAGGATAAGCGGACAGG	GCGGTTTGGTCAGATAAAGGT
NNMT	CCGGGAGGCAGTAGAGGC	GTCCTTCGTTGTTGGCCAT
IGFLS	TCTGCAGGGCGAAGTCC	
KLOTHO	AGCCATTATACCACCATCCTTG	GTCGGTCATTTCTTGCACTTCTA
P4AH1	TGGATACCCATTTGTTGCCA	
SLC16A1	TGCTGGAGCCCTCATGC	TTCCAGCTTTCTCAAGGGATG
SRD5A1	TACGTATTCAAATAAGCCTCCCCT	
SCD	TCAAAACAGTGTGTTCGTTGC	CATAAGGACGATATCCGAAGAGG
FADS1	CAGGCCACATGCAATGTC	ATCTAGCCAGAGCTGCCCTG
FADS2	GGCTCTCCAGGAACCTGATG	
FASN	GGCAAATTCGACCTTTCTCAG	AGGACCCCGTGGAATGTC
DGAT2	ACGGCCTTACCTGGCTACA	AGACATCAGGTACTCCCTCAACAC
ADPN	CCTCCAGGTCCCAAATGCC	CCAGTCCTGCTCAGGTGTGC
AKR1B10	GGCCTGTAACGTGTTGC	ATGGGACATGAGTGGAGG
SREBP1c	CATGGATTGCACATTTGAAG	CAGAGAGGAGGCCAGAGAA
FABP	GATCCAAAACGAATTCACGG	ATTGTCACCTTCCAACTGAACC
GAPDH	CCACCTTTGACGACGCTGGG	CATACCAGGAAATGAGCTTGACA

synthesized using 1 μg RNA and PowerScript reverse transcriptase (Clontech, Mountain View, CA) and oligo-deoxythymidine primers (Invitrogen) and was subjected to real-time qRT-PCR following the manufacturer's instructions. Genes were amplified with a set of gene-specific primers (Table 3) and SYBR Green PCR mix in a PRISM 7700 sequence detector (Applied Biosystems, Tokyo, Japan). These primers were capable of amplifying human, but not mouse, genes. PCR products were monitored during amplification. All data were calculated by the comparative threshold cycle (Ct) method (22). Occupancy rates of h-hepatocytes in h-hepatocyte regions ranged from 70–95% (Table 2). Contamination of m-hepatocytes did not affect RT-PCR results of human gene expression because each gene's expression level was normalized against h-GAPDH.

Responsiveness of h-hepatocytes$_{chimeric\ mouse}$ to h-GH and h-IGF-I

Hepatocytes synthesize and secrete IGF-I when GH receptors are activated by GH (23). To determine whether h-GH directly regulates GH-responsive genes or h-IGF-I, h-hepatocytes$_{6YF}$ (9×10^5 cells) from three chimeric mice were cultured in 1.8-cm Matrigel-coated dishes in DMEM as previously reported (24), and 4 h later, they were exposed with 0, 5, and 50 ng/ml h-GH or 50 and 500 ng/ml h-IGF-I for an additional 24 and 48 h and harvested in RLT buffer to prepare total RNA for real-time qRT-PCR.

Gene enrichment analysis

Gene and gene ontology (GO) information were collected from NCBI build 37.1 (ftp://ftp.ncbi.nlm.nih.gov/gene/DATA/gene2go.gz) and The Gene Ontology (http://www.geneontology.org/ontology/gene_ontology.obo) sites, respectively. Pathway information was collected from KEGG (ftp://ftp.genome.jp/pub/kegg/pathway/organisms/hsa/hsa_gene_map.tab) and Ingenuity Pathways Analysis (IPA) software (Ingenuity Systems, Redwood City, CA). The gene enrichment analysis was performed using only GO and pathway groups where at least two genes or more were assigned.

Statistics

Microarray data were evaluated by the Welch's t test (two-sided). The gene enrichment analysis was calculated using Fisher's exact test and corrected with Benjamini-Hochberg's false discovery rate (25). The significance of overlap between two groups of transcripts was determined using Fisher's exact test. Log$_{10}$-transformed data obtained in real-time qRT-PCR analysis of in vivo and in vitro studies were analyzed among groups by ANOVA. When the overall F statistics were significant, significance was determined by the Scheffé's test with significance level $\alpha = 0.05$.

Results

Lipid accumulation in chimeric mouse livers

Hepatocytes$_{6YF}$ were transplanted to uPA/SCID mice, and the process of h-hepatocyte repopulation in host livers was visualized using hematoxylin- and eosin-stained histological sections. Vacuoles appeared in the cytoplasm of donor h-hepatocytes approximately 70 d after transplantation and gradually increased in numbers and sizes thereafter (Fig. 1A, a and b). To test whether these vacuoles represent lipid deposits, 36 chimeric mice$_{6YF}$ were killed 48–111 d after transplantation (five before 60 d, 28 between 70 and 90 d, and three after 90 d) for ORO staining of liver sections (Fig. 1B). Most of the chimeric liver h-hepatocytes became ORO$^+$ approximately 70 d after transplantation. The steatosis level was quantified by the size and frequency of ORO$^+$ lipid droplets from grade 0 (Fig. 1Ba) to grade 3 (Fig. 1Bd) and plotted against post-transplantation days (Fig. 1C). Among five livers before 60 d of transplantation, one and four livers were of grade 0 and 1, respectively (Fig. 1C). Most of the livers between 70 and 90 d were of grade 1 (11 of 28 mice) and grade 2

(nine of 28). All three livers after 90 d were of grade 3, showing a good correlation of the steatosis level with post-transplantation duration (~50–110 d). h-IGF-I serum levels of chimeric mice$_{6YF}$, a measure of h-GH level, were under a detection limit of 9.4 ng/ml (n = 3), which supported our previous study that chimeric mouse h-hepatocytes were h-GH deficient (6). Therefore, we considered h-GH deficiency as an etiological factor in the observed hepatic lipogenesis.

Improvement of liver steatosis in chimeric mice by h-GH

To examine the relationship of steatosis with-GH-deficiency, five chimeric mice$_{6YF}$ at different time points after transplantation were infused with h-GH during the last 2 wk before killing (one mouse was killed at 83 d, three at 84 d, and the remaining one at 89 d) and were used as h-GH-treated chimeric mice. Twenty-eight of 36 chimeric mice$_{6YF}$ that were used in the experiment shown in Fig. 1C and killed 70–90 d after transplantation served as controls. The h-IGF-I serum level rose to 72.5 ± 9.4 ng/ml (n = 3) in h-GH-treated mice, a level comparable to that in normal human sera, proving the effectiveness of the h-GH treatment. Serial histological sections were immunostained for h-CK8/18 to identify h-hepatocytes (Fig. 2, A and B) and stained with ORO (Fig. 2, C and D). ORO$^+$ droplets were present in the control mouse h-hepatocytes (Fig. 2, A and C) but were not in h-GH-treated ones (Fig. 2, B and D). Some host m-hepatocytes also contained small cytoplasmic ORO$^+$ droplets (Fig. 2, A and C), probably due to uPA damage because even after h-GH treatment, these lipid droplets remained (Fig. 2, B and D). Steatosis grading on liver sections showed that most of the control mouse livers (93%) were of grade 1–3: 39, 32, and 21% for grades 1, 2, and 3, respectively (Fig. 2E). All h-GH-treated livers were of grade 0. Therefore, we concluded that h-GH plays a critical role in the etiology of human liver steatosis.

h-GH-induced changes in gene expression profiles at the hepatocyte level

Hepatocytes were isolated from three h-GH-untreated chimeric mice$_{9MM}$ 72–101 d after transplantation (nos. 1–3) and three h-GH-treated chimeric mice$_{9MM}$ 75 d after transplantation (nos. 4–6) for microarray analysis (Table 2). We found 15,826 positive transcripts (29%) in 54,675 spotted transcripts in either h-GH-untreated or -treated h-hepatocytes$_{chimeric liver}$. Among these, 229 (1.4%) and 269 (1.7%) transcripts showed more than 2-fold higher and lower expression levels in h-GH-treated than -untreated h-hepatocytes, respectively. Statistical evaluation at $P < 0.05$ selected 58 genes (82 transcripts) from 229 transcripts as

up-regulated in h-GH-treated h-hepatocytes$_{chimeric mouse}$. Similarly, 33 genes (37 transcripts) were selected from the 269 transcripts as down-regulated genes.

Gene enrichment analysis on transcripts showing more than 2-fold changes selected the significantly overrepresented (GH-induced and -suppressed) GO terms and pathways including GH signaling, IGF-I receptor binding, response to hormone stimulus, lipid biosynthetic process, and aging (Table 4 and Supplemental Table 1, published on The Endocrine Society's Journals Online web site at http://endo.endojournals.org).

TABLE 4. Extracted significantly overrepresented GO terms and pathways

Pathway, or GO term	P value	B-H FDR q-value
Hepatocyte level		
Pathway		
GH signaling	0.000244	0.00830
GO molecular function		
IGF receptor binding	3.77×10^{-5}	0.00464
GO biological process		
Response to hormone stimulus	4.30×10^{-5}	0.00556
Lipid biosynthetic process	0.000898	0.0251
Lipid metabolic process	0.00122	0.0284
Aging	0.00288	0.0334
Regulation of fatty acid biosynthetic process	0.00353	0.0358
Regulation of lipid metabolic process	0.0241	0.0947
Tissue level		
Pathway		
Biosynthesis of unsaturated fatty acids	2.78×10^{-5}	0.000584
GH signaling	0.0116	0.0612
GO molecular function		
Stearoyl-coenzyme A 9-desaturase activity	8.78×10^{-5}	0.00382
IGF receptor binding	0.00256	0.0500
GO biological process		
Fatty acid metabolic process	0.000189	0.00585
Lipid metabolic process	0.000739	0.0133
Oxidation reduction	0.00312	0.0288
Response to hormone stimulus	0.00468	0.0346
Aging	0.00627	0.0392
Unsaturated fatty acid biosynthetic process	0.0186	0.0692

B-H FDR, Benjamini-Hochberg's false discovery rate.

h-GH-induced changes in gene expression profiles at the liver tissue level

Identical microarray analysis was performed at the liver tissue level with six chimeric mice$_{6YF}$ (Table 2), with half (nos. 1–3) being used as controls and the other half (nos. 4–6) as h-GH-treated mice. In this analysis, h-hepatocyte-repopulated regions were dissected from liver tissues of these animals and used as h-liver$_{chimeric\ mouse}$ as RNA sources for microarray analysis in which 54,675 transcripts were spotted as in the case of the hepatocyte-level analysis. Transcripts positive for either h-GH-untreated or -treated h-liver$_{chimeric\ mouse}$ were 18,210 (33%) transcripts, among which 146 (0.8%) and 237 (1.3%) transcripts were expressed at more than 2-fold higher and lower levels, respectively, in h-GH-treated tissues than in h-GH-untreated controls. Through statistical evaluation ($P < 0.05$), we identified 43 genes (64 transcripts) and 55 genes (76 transcripts) as up- and down-regulated genes by h-GH from the 146 and 237 transcripts, respectively.

Gene enrichment analysis on transcripts showing more than 2-fold changes selected the significantly overrepresented (GH-induced and -suppressed) GO terms and pathways including biosynthesis of unsaturated fatty acids, GH signaling, stearoyl-coenzyme A desaturase (SCD) activity, IGF receptor binding, oxidoreductase activity, fatty acid metabolic process, aging were significantly changed (Table 4 and Supplemental Table 2).

In summary, we selected 58 up-regulated and 33 down-regulated genes from the h-hepatocyte-level assay and 43 up-regulated and 55 down-regulated genes from the h-liver tissue-level assay. From them, we chose genes that were commonly up- and down-regulated at both the hepatocyte and liver tissue levels. As a result, 14 up-regulated genes (23 transcripts) and four down-regulated genes (five transcripts) were finally identified as more reliable candidates for h-GH-responsive genes as listed in Table 5, in which the expression ratios at the hepatocyte level [h-GH-treated h-hepatocytes$_{chimeric\ mouse}$ vs. h-GH-untreated h-

TABLE 5. h-GH-regulated genes

Affymetrix ID	Gene symbol	Accession Number	Gene name	Cell level, treated/untreated		Tissue level, treated/untreated	
				Microarray	RT-PCR[a]	Microarray	RT-PCR[a]
Up-regulated							
209988_s_at	ASCL1	NM_004316.3	Achaete-scute complex-like 1	123.39	–	151.42	–
209540_at	IGF1[b]	AU144912	IGF-I	179.66	159.83	34.19	35.45
203373_at	SOCS2[b]	NM_003877	Suppressor of cytokine signaling 2	39.01	73.79	13.91	53.20
202237_at	NNMT[b]	NM_006169	Nicotinamide N-methyltransferase	46.02	40.09	14.28	20.79
205978_at	KL[b]	NM_004795	Klotho	39.90	22.50	6.58	8.45
207543_s_at	P4HA1[b]	NM_000917	Procollagen-proline, 2-oxoglutarate 4-dioxygenase, α-polypeptide I	15.17	11.99	9.69	9.03
203498_at	DSCR1L1	NM_005822	Down syndrome critical region gene 1-like 1	5.77	–	4.06	–
215712_s_at	IGFALS[b]	AW338791	IGF-binding protein, acid labile subunit	5.29	9.49	7.29	13.63
209967_s_at	CREM	D14826	cAMP-responsive element modulator	4.41	–	2.76	–
207256_at	MBL2	NM_000242	Mannose-binding lectin 2, soluble	3.44	–	2.09	–
222108_at	AMIGO2	AC004010	Adhesion molecule with Ig-like domain 2	2.89	–	2.84	–
201309_x_at	C5orf13	U36189	Chromosome 5 open reading frame 13	2.75	–	3.47	–
202234_s_at	SLC16A1[b]	BF511091	Solute carrier family 16, member 1	2.74	2.29	4.14	3.84
211056_s_at	SRD5A1[b]	BC006373	Steroid-5-α-reductase, α-polypeptide 1	2.29	1.99	2.03	1.72
Down-regulated							
208964_s_at	FADS1[b]	AL512760	Fatty acid desaturase 1	0.43	0.51	0.36	0.29
219295_s_at	PCOLCE2	NM_013363	Procollagen C-endopeptidase enhancer 2	0.37	–	0.45	–
206561_s_at	AKR1B10[b]	NM_020299	Aldo-keto reductase family 1, member B10	0.22	0.22	0.19	0.13
202628_s_at	SERPINE1	NM_000602	Serine proteinase inhibitor, clade E, member 1	0.17	–	0.28	–

Treated indicates h-GH-treated chimeric mouse, whereas untreated indicates h-GH-untreated chimeric mouse. –, Not determined.

[a] The expression level of each gene was divided with that of h-GAPDH.

[b] Gene expression levels were determined by both microarray assay and real-time qRT-PCR.

hepatocytes$_{\text{chimeric mouse}}$ (cell level, treated/untreated)] and at the tissue level [h-GH-treated h-liver$_{\text{chimeric mouse}}$ *vs.* -untreated h-liver$_{\text{chimeric mouse}}$ (tissue level, treated/untreated)] are presented for each gene. *P* values for overrepresentation of the overlapping genes (up- and down-regulated genes in both hepatocytes and liver tissue levels) were 5.34 × 10^{-9} and 1.92 × 10^{-9}, respectively, which indicates the significance of the overlapping.

The microarray assay's results were validated by real-time qRT-PCR using RNA extracted from the sources shown in Table 2 on arbitrarily selected eight and three genes from the above final 14 h-GH-up- and four h-GH-down-regulated genes, respectively: *IGF-I*, suppressor of cytokine signaling 2 (*SOCS2*), nicotinamide *N*-methyltransferase (*NNMT*), *KL*, *P4HA1*, *IGFALS*, solute carrier family 16/member 1 (*SLC16A1*), and steroid-5-α-reductase and α-polypeptide 1 (*SRD5A1*) as h-GH-up-regulated genes and fatty acid desaturase (*FADS1*) and aldo-keto reductase family 1/member B10 (*AKR1B10*) as h-GH-down-regulated genes. The expression ratios (treated/untreated) calculated from the qRT-PCR results are included in Table 5, which well support the microarray data, indicating the reliability of the microarray data.

There was the possibility that mouse transcripts were also included as the cDNAs hybridized in the currently adopted microarray assay. To check this possibility, pooled cDNAs of three uPA/SCID mouse livers were subjected to the microarray with 54,675 cDNA spots, which gave a result that 5,643 of 54,675 transcripts (10.3%) were positive. Sixteen genes among the genes listed in Table 5 were not found in these positive genes, but two genes, *SOCS2* and *IGFALS*, both h-GH-up-regulated genes, were found there. Considering that the cross-hybridized signals were less than 10% of those in the GH-untreated hepatocytes$_{\text{chimeric mouse}}$ and the contamination of mouse hepatocytes in the h-hepatocyte preparation used in the present study was less than 10% (Table 2, 9MM nos. 1–6), we concluded that their ratios of treated to untreated genes were high enough to include them as h-GH-regulated genes in the present study. This conclusion was further validated by measuring m-Alb mRNA expression levels in the h-liver$_{\text{chimeric mouse}}$. Real-time qRT-PCR was performed for RNAs isolated from h-liver$_{\text{chimeric mouse}}$ (Table 2, 6YF nos. 1–6) using a set of m-Alb primers. The result showed that m-Alb expression levels in the h-liver$_{\text{chimeric mouse}}$ were 0.5 ± 0.2% of those of the uPA/SCID mouse liver. As a whole, it can be said that the cross-reactivity does not affect the results in the present study.

Improvement of gene expression by h-GH

Real-time qRT-PCR was performed for livers of h-GH-untreated chimeric, h-GH-treated chimeric mice,

and humans, the last of which accurately reflect the physiology of h-GH endocrine regulation. The h-GH-untreated and -treated h-hepatocytes$_{\text{chimeric mouse}}$ were isolated from nos. 1–3 and nos. 4–6 of chimeric mice$_{9\text{MM}}$, respectively (Table 2). The h-GH-untreated and -treated h-liver$_{\text{chimeric mouse}}$ were isolated from nos. 1–3 and nos. 4–6 of chimeric mice$_{6\text{YF}}$, respectively (Table 2). The h-hepatocytes$_{\text{human}}$ and h-liver$_{\text{human}}$ were isolated from four (28YM, 57YM, 25YF, and 61YF) and three (28YM, 25YF, and 61YF) donors, respectively (Table 1). Expression levels in h-hepatocytes$_{\text{chimeric mouse}}$ and h-liver$_{\text{chimeric mouse}}$ under h-GH-untreated and -treated conditions were divided by the h-hepatocyte$_{\text{human}}$ and the h-liver$_{\text{human}}$, respectively, which is shown as the hepatocyte ratio (*white bars*) and liver-tissue ratio (*black bars*), respectively (Fig. 3). The ratios are used as measures of the extent of difference/closeness of the gene expression level in h-GH-treated or -untreated chimeric livers from/to that in human liver. If h-GH improves gene expressions in chimeric mouse livers, ratios for h-GH-up-regulated genes in h-GH-untreated and -treated chimeric liver are expected to be less than 1 and approximately 1, respectively, and ratios for h-GH-down-regulated genes in h-GH-untreated and -treated chimeric liver are expected to be more than 1 and approximately 1, respectively.

Expression levels of a total of eight h-GH-up-regulated genes were compared between h-GH-untreated and -treated chimeric mice at both hepatocyte and liver tissue levels. The results of the h-GH-up-regulated genes are shown in Fig. 3A. Generally, the expressions of the genes, except *KL*, were significantly suppressed in the absence of h-GH at both the hepatocyte and liver tissue levels. Expression in h-GH-treated cases was similar to that in human livers: *IGF-I* and *P4AH1* at the tissue level and *IGFALS* and *SLC16A1* at both levels. *KL* expression in h-GH-untreated chimeric mice was similar to that in human livers at both levels, and h-GH treatment markedly increased expression over that in human livers at both levels, suggesting that its expression is greatly up-regulated by GH. *In vivo*, h-GH-up-regulated genes of human livers are likely positively induced by GH.

Our results on suppression of spontaneous lipogenesis by GH (Fig. 2) and a reported relationship between GH-responsive genes and lipogenesis-related genes (26) suggest an association between the h-GH-responsive genes listed in Table 5 and the observed hepatic lipogenesis. Gene enrichment analysis showed that h-GH-responsive genes were enriched as those involved in the lipid synthesis process, lipid metabolic process, and regulation of fatty acid biosynthetic process (Table 4). Of the two down-regulated genes, *FADS1* is known to be lipogenesis related (27), and *AKR1B10* was recently reported to regulate fatty acid synthesis (28). Five genes were additionally cho-
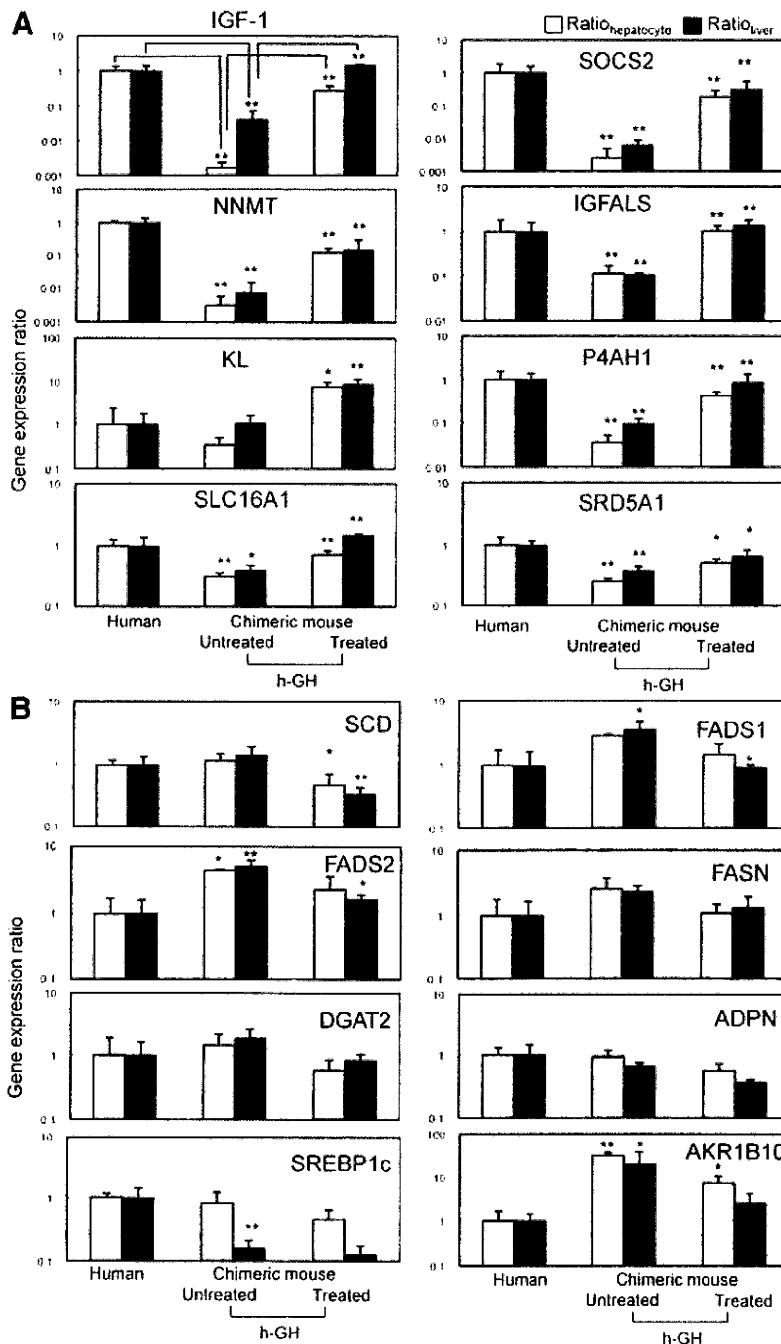
FIG. 3. Regulation of gene expression in h-hepatocytes_chimeric mouse by h-GH at the hepatocyte and liver tissue levels. Six chimeric mice_9MM and six chimeric mice_6YF were produced (Table 2); half of each group (nos. 1–3 for both the chimeric mice_9MM and chimeric mice_6YF) served as control animals, and the remaining half (nos. 4–6 for both the chimeric mice_9MM and chimeric mice_6YF) were treated with h-GH. h-Hepatocytes_chimeric mouse and h-livers_chimeric mouse were isolated from the former and latter chimeric mice, respectively. h-Hepatocytes_human and h-livers_human were also isolated from four (25YF, 28YM, 57YM, and 61YF) and three (25YF, 28YM and 61YF) human donors, respectively (Table 1). RNA was isolated from the hepatocytes and liver tissue for real-time qRT-PCR analysis. qRT-PCR was performed for eight h-GH-up-regulated (A) and eight lipogenesis-related (B) genes. The expression level of each gene was normalized against that of h-GAPDH. The expression level of h-GH-untreated h-hepatocytes_chimeric mouse and h-GH-treated h-hepatocytes_chimeric mouse was divided by that of h-hepatocytes_human (ratio_hepatocyte). Similarly, the expression level of h-livers_chimeric mouse was divided by that of h-livers_human (ratio_liver). White and black bars represent the ratio_hepatocyte and the ratio_liver, respectively. Each value represents the mean ± SD. Asterisks above bars of untreated chimeric mouse show significance between human and GH-untreated chimeric mouse. Asterisks above bars of treated chimeric mouse show significance between human and GH-treated chimeric mouse. *, $P < 0.05$; **, $P < 0.01$.

sen to examine the relationship between h-GH-down-regulated genes and known lipogenic genes from previous studies: FADS2 (27), SCD (29), FASN (30), diacylglycerol acryltransferase 2 gene (DGAT2) (31), and the adiponutrin gene [ADPN (32), currently known as PNPLA3 (33)]. These genes were included as h-GH-down-regulated genes at either the hepatocyte or liver tissue level in the microarray assay; FADS2 and SCD were significantly ($P < 0.05$) down-regulated only at the liver tissue level, FASN was insignificantly (>2-fold) down-regulated only at the hepatocyte level, DGAT2 was insignificantly (>2-fold) down-regulated only at the hepatocyte level, and ADPN significantly ($P < 0.05$) decreased its expression only at the hepatocyte level. Two known GH-inducible lipogenesis-related genes, SREBP1c (34–36) and fatty acid-binding protein gene (FABP) (24, 37), were also chosen from previous studies.

Expression of a total of nine genes was compared between human livers and h-GH-untreated and -treated chimeric mice at both hepatocyte and liver tissue levels as above. Results for lipogenesis-related genes are shown in Fig. 3B. Ratios of three genes, FADS1 (significant at tissue level), FADS2 (significant at both levels), and AKR1B10 (significant at both levels), were higher in the h-GH-untreated chimeric mice compared with humans, and h-GH treatment lowered the ratios of SCD (significant at both levels), FADS1 (significant at tissue level), FADS2 (significant at tissue level), and AKR1B10 (significant at hepatocyte level). Although not significantly, ratios of FASN and DGAT2 were also higher in the h-GH-untreated chimeric mice compared with humans and decreased by h-GH treatment. ADPN expression in h-GH-untreated chimeric mice was close to that in humans at both levels, and h-GH treatment decreased ratios (insignificant). Thus, it is most likely that these lipogenesis-related genes are down-regulated by h-GH. Ratios of SREBP1c (Fig.

3B) and *FABP* (data not shown) genes did not show any meaningful changes by h-GH at either the hepatocyte or liver tissue level under the observed endocrinological conditions, although *SREBP1* expression was significantly lower at tissue levels in h-GH-untreated chimeric mice compared with human.

Deletion of GH receptor gene (*GHR*) in mice resulted in an increase of insulin receptor gene (*IRS*) expression (38) and a reduction of plasma levels of IGF-I, insulin, and glucose, implying that the mice increased insulin sensitivity (39, 40). These studies suggested the possibility that chimeric mice are insulin sensitive. Thus, we examined whether chimeric mice are insulin sensitive by determining the expression levels of h-*GHR* and h-*IRS*. Real-time qRT-PCR analysis showed that h-*GHR* and h-*IRS* expression levels in chimeric mice were similar or higher than humans, and h-GH administration of chimeric mice did not affect these observed expression levels. However chimeric mice did not show any sign of insulin resistance or sensitivity in a sugar tolerance test (data not shown). As a whole, we currently consider that chimeric mice are not insulin sensitive.

In vitro effects of h-GH on gene expressions in h-hepatocytes

We asked whether the aforementioned effects of h-GH on the h-GH-up-regulated gene and lipogenic gene expression in chimeric mouse livers *in vivo* are reproducible *in vitro*. h-Hepatocytes$_{6YF}$ isolated from three chimeric mice with RI$_{Alb}$ higher than 95% at 70–80 d after transplantation were cultured for 24 and 48 h in the presence and absence of h-GH and h-IGF-I, followed by determination of expression levels of the eight h-GH-up-regulated genes by real-time qRT-PCR (Fig. 4A). Expression of *IGF-I*, *SOCS2*, *NNMT*, *IGFALS*, and *P4AH1* were significantly increased by h-GH in a dose-dependent manner, but h-IGF-I did not enhance expression of the genes, indicating the direct the action of h-GH on the expression of these genes. The remaining three genes (*KL*, *SLC16A1*, and *SRD5A1*) were not responsive to h-GH or h-IGF-I.

Results for lipogenic genes (*SCD*, *FADS1*, *FADS2*, *FASN*, *DGAT2*, *ADPN*, *AKR1B10*, and *SREBP1c*) are shown in Fig. 4B. Only *FADS1*, *DGAT2*, *SREBP1c*, and *AKR1B10* significantly decreased the expression at 24 or 48 h exposure of 50 ng/ml h-GH. Although insignificant, *SCD*, *FADS2*, and *FASN* were decreased by GH exposure. The expression levels of the eight genes did not significantly change by h-IGF-I.

Discussion

GH regulation of lipogenic genes has been generally studied using rodents (34–37, 41–43), and no suitable animal model whose liver mimics the human liver has been available. Currently, we propose an h-hepatocyte-bearing chimeric mouse as one such model, in which heavy lipid accumulation spontaneously takes place in h-hepatocytes more than 2 months after transplantation but does not when the animals are administered h-GH. Using this model, we demonstrated that h-GH deficiency is a cause of the steatosis and identified 14 and four genes as h-GH-up- and -down-regulated genes at both the hepatocyte and liver tissue level, in which three new lipogenic genes (*FADS1*, *FADS2*, and *AKR1B10*) were included. Regarding h-GH-down-regulated genes, we characterized an additional seven lipogenic genes, although these genes were h-GH down-regulated only at the hepatocyte level or liver tissue level. *FADS1*, *FADS2*, and *AKR1B10* were included in these seven genes and were significantly up-regulated in the chimeric mouse liver compared with human liver, but their expression was down-regulated by h-GH. Thus, it is suggested that these genes participate in the spontaneous steatosis observed in the chimeric mouse liver.

Results of previous studies indicated the presence of species differences in GH responsiveness of lipogenic genes between rats and mice. *SREBP-1c*, a known transcription factor of lipogenic genes, and its target genes, *FASN* and *SCD-1*, appear to be GH up-regulated in rats; hypophysectomy decreases expression of these genes, and the infusion of the rats with GH improved their expression to the original levels (34, 35). By contrast, a study with GH-transgenic technology showed that the same genes were down-regulated in mice (44). Recent microarray analysis supported such species differences; GH treatment suppressed *SCD* gene expression level in hypophysectomized mouse livers (42) but not in hypophysectomized rat livers (41). There are also differences regarding GH responsiveness of lipogenic genes between *in vitro* and *in vivo* studies; the above cited authors showed in a study with primary cultures of rat hepatocytes *SCD1* as GH up-regulated, *FASN* as GH down-regulated, and *SREBP-1c* as GH nonresponsive (34). In the present study, expression of h-*SCD*, but not h-*SREBP-1c*, was reduced by h-GH administration to the chimeric mice, and h-*FABP* expression was not affected by h-GH, which was different from a rat study (34). h-*FADS1*, h-*FADS2*, and h-*AKR1B10* were down-regulated in the present study, but they did not report them as GH-down-regulated genes in rodent studies. In addition, AGHD patients show fatty liver and nonalcoholic steatohepatitis (NASH) (8), and GH treatment improved the symptoms (13, 14). However, studies using hypophysectomized rodents did not report such changes (34, 35, 41, 42).

The serum concentration of GH is low in nonalcoholic fatty liver disease (NAFLD) patients (15), and *NNMT* and
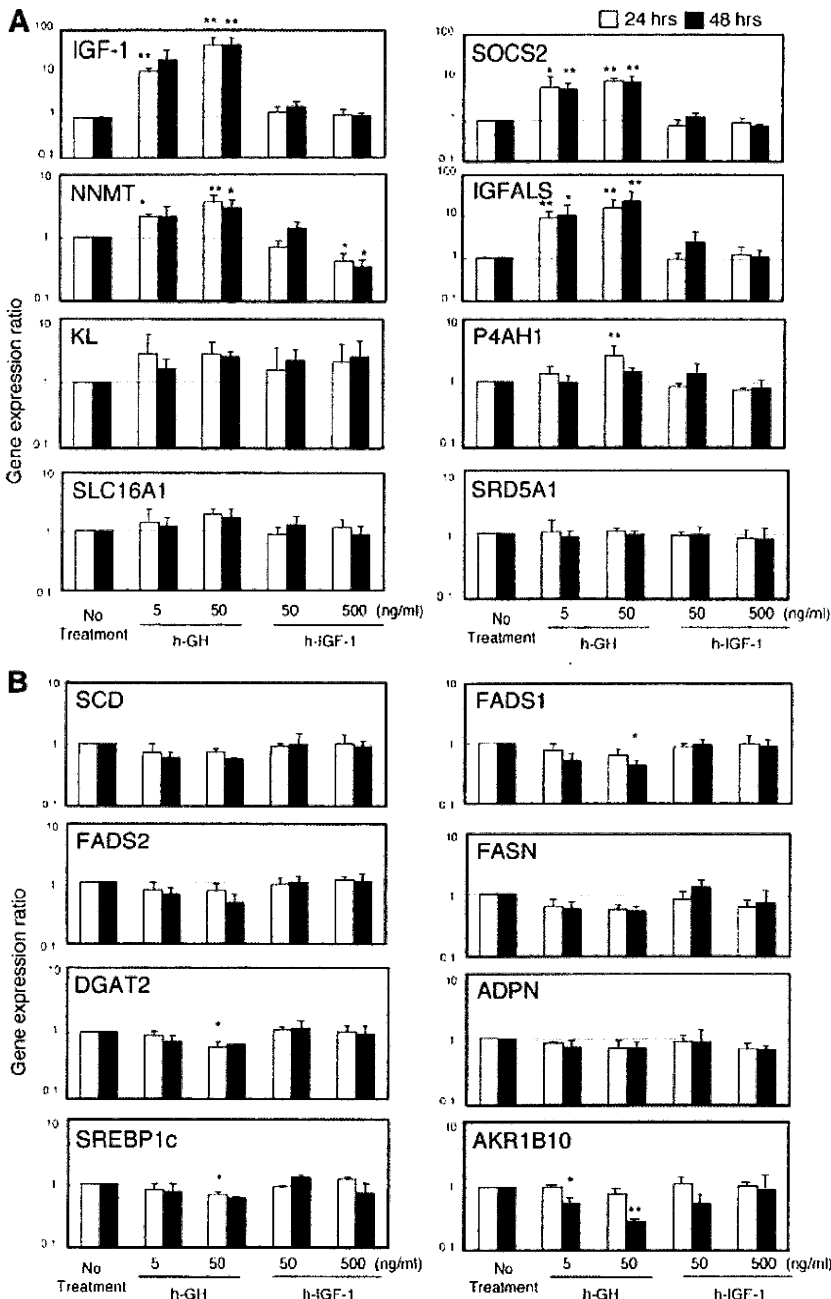
FIG. 4. *In vitro* effects of h-GH and h-IGF-I on the expression level of lipogenesis genes. h-Hepatocytes$_{GVF}$ were cultured with 0, 5, or 50 ng/ml h-GH or 50 or 500 ng/ml h-IGF-I for 24 and 48 h and subjected to RNA isolation to perform real-time qRT-PCR analysis for eight h-GH-up-regulated genes (A) and eight lipogenesis-related genes (B). The expression level of each gene was normalized against that of h-*GAPDH*. The gene expression level of h-hepatocytes treated with h-GH or h-IGF-I was divided by that of untreated h-hepatocytes. White and black bars represent 24 and 48 h, respectively. Each value represents the mean ± SD. Asterisks above a bar show significance between no treatment and each dose of h-GH or h-IGF-I treatment. *, $P < 0.05$; **, $P < 0.01$.

dependent manner. Thus, chimeric mice could be particularly useful as an NAFLD/NASH mouse model, with the genes identified in this study serving as therapeutic target genes for NAFLD patients.

Among 14 h-GH-up-regulated genes characterized in this study, eight genes (*IGF-I*, *SOCS2*, *NNMT*, *P4HA1*, *IGFALS*, *MBL2 AMIGO2*, and *SRD5A1*) are known GH-up-regulated genes (23, 41–43, 45), but the remaining six h-GH-up-regulated genes (*ASCL1*, *KL*, *DSCR1L1*, *CREM*, *C5orf13*, and *SLC16A1*) have never been reported as up-regulated genes. Roles of these newly identified GH-up-regulated genes in the human liver could be further investigated using the chimeric mice.

The protein Klotho is known to inhibit insulin/IGF-I signaling, which likely increases resistance to oxidative stress and potentially contributes to its claimed anti-aging properties (46). In the present study, *KL* expression levels were similar in human and chimeric mouse livers, but h-GH markedly induced *KL* gene expression in the latter. The findings of the present study suggested a mutual regulatory mechanism(s) between the two genes: *h-GH* might play a role in the anti-aging process through the *KL* induction.

We were able to propagate h-hepatocytes in chimeric mouse livers, which could solve the problem of a quite limited availability of human hepatocytes for research purposes. In fact, in the present study, we showed the usefulness of chimeric mouse-derived h-hepatocytes for *in vitro* study by testing the effects of h-GH or h-IGF-I on expression levels of eight lipogenic genes that had been up-regulated in chimeric mouse liver *in vivo*. We were able to answer a question of whether h-GH and h-IGF-I in combination directly or indirectly induce such changes in gene expression. Hepatocytes in conventional two-dimensional culture do not generally recapitulate gene expression profiles observed under *in vivo* conditions. In the present study, hepatocytes were three-

IGFALS are up-regulated in NASH patients (47). Fatty livers of chimeric mice in the present study appreciably reproduce expression profiles of these known NAFLD/NASH-associated genes. We showed that h-GH regulates h-*SCD* and other lipogenesis-related genes, including h-*FADS1*, h-*FADS2*, and h-*AKR1B10* in a h-*SREBP1*-in-

dimensionally cultured on Matrigel (spheroid culture), which allowed them to express gene expression closer to *in vivo* conditions as reported previously (48).

We resected h-hepatocyte regions from chimeric livers for microarray analysis and real-time RT-PCR. The gene expression profiles determined using the dissected regions were similar to those determined using the isolated h-hepatocytes$_{chimeric\ mouse}$. This finding also indicates the usability of chimeric mouse liver tissues as an alternative RNA source to h-hepatocytes, whose isolation is time consuming and laborious.

In conclusion, the present study shows that chimeric mice could overcome the species difference between experimental animals and humans, and therefore, these mice are useful for investigating the mechanism of the action of GH on h-hepatocytes *in vivo* and role of GH in NAFLD/NASH.

Acknowledgments

References

1. Tateno C, Yoshizane Y, Saito N, Kataoka M, Utoh R, Yamasaki C, Tachibana A, Soeno Y, Asahina K, Hino H, Asahara T, Yokoi T, Furukawa T, Yoshizato K 2004 Near-completely humanized liver in mice shows human-type metabolic responses to drugs. Am J Pathol 165:901–912

2. Yoshizato K, Tateno C 2009 A human hepatocyte-bearing mouse: an animal model to predict drug metabolism and effectiveness in humans. PPAR Res 2009:476217

3. Yoshizato K, Tateno C 2009 In vivo modeling of human liver for pharmacological study using humanized mouse. Expert Opin Drug Metab Toxicol 5:1435–1446

4. Katoh M, Matsui T, Okumura H, Nakajima M, Nishimura M, Naito S, Tateno C, Yoshizato K, Yokoi T 2005 Expression of human phase II enzymes in chimeric mice with humanized liver. Drug Metab Dispos 33:1333–1340

5. Nishimura M, Yoshitsugu H, Yokoi T, Tateno C, Kataoka M, Horie T, Yoshizato K, Naito S 2005 Evaluation of mRNA expression of human drug-metabolizing enzymes and transporters in chimeric mouse with humanized liver. Xenobiotica 35:877–890

6. Masumoto N, Tateno C, Tachibana A, Utoh R, Morikawa Y, Shi-

mada T, Momisako H, Itamoto T, Asahara T, Yoshizato K 2007 GH enhances proliferation of human hepatocytes grafted into immunodeficient mice with damaged liver. J Endocrinol 194:529–537

7. Souza SC, Frick GP, Wang X, Kopchick JJ, Lobo RB, Goodman HM 1995 A single arginine residue determines species specificity of the human growth hormone receptor. Proc Natl Acad Sci USA 92:959–963

8. Brunt EM 2010 Pathology of nonalcoholic fatty liver disease. Nat Rev Gastroenterol Hepatol 7:195–203

9. Johannsson G, Bengtsson BA 1999 Growth hormone and the metabolic syndrome. J Endocrinol Invest 22:41–46

10. Ichikawa T, Nakao K, Hamasaki K, Furukawa R, Tsuruta S, Ueda Y, Taura N, Shibata H, Fujimoto M, Toriyama K, Eguchi K 2007 Role of growth hormone, insulin-like growth factor 1 and insulin-like growth factor-binding protein 3 in development of non-alcoholic fatty liver disease. Hepatol Int 1:287–294

11. Ichikawa T, Hamasaki K, Ishikawa H, Ejima E, Eguchi K 2003 Non-alcoholic steatohepatitis and hepatic steatosis in patients with adult onset growth hormone deficiency. Gut 52:914

12. Adams LA, Feldstein A, Lindor KD, Angulo P 2004 Nonalcoholic fatty liver disease among patients with hypothalamic and pituitary dysfunction. Hepatology 39:909–914

13. Takahashi Y, Iida K, Takahashi K, Yoshioka S, Fukuoka H, Takeno R, Imanaka M, Nishizawa H, Takahashi M, Seo Y, Hayashi Y, Kondo T, Okimura Y, Kaji H, Kitazawa R, Kitazawa S, Chihara K 2007 Growth hormone reverses nonalcoholic steatohepatitis in patients with adult growth hormone deficiency. Gastroenterology 132:938–943

14. Lonardo A, Carani C, Carulli N, Loria P 2006 'Endocrine NAFLD' a hormonocentric perspective of nonalcoholic fatty liver disease pathogenesis. J Hepatol 44:1196–1207

15. Lonardo A, Loria P, Leonardi F, Ganazzi D, Carulli N 2002 Growth hormone plasma levels in nonalcoholic fatty liver disease. Am J Gastroenterol 97:1071–1072

16. Meuleman P, Vanlandschoot P, Leroux-Roels G 2003 A simple and rapid method to determine the zygosity of uPA-transgenic SCID mice. Biochem Biophys Res Commun 308:375–378

17. Jeschke MG, Herndon DN, Finnerty CC, Bolder U, Thompson JC, Mueller U, Wolf SE, Przkora R 2005 The effect of growth hormone on gut mucosal homeostasis and cellular mediators after severe trauma. J Surg Res 127:183–189

18. Utoh R, Tateno C, Yamasaki C, Hiraga N, Kataoka M, Shimada T, Chayama K, Yoshizato K 2008 Susceptibility of chimeric mice with livers repopulated by serially subcultured human hepatocytes to hepatitis B virus. Hepatology 47:435–446

19. Utoh R, Tateno C, Kataoka M, Tachibana A, Masumoto N, Yamasaki C, Shimada T, Itamoto T, Asahara T, Yoshizato K 2010 Hepatic hyperplasia associated with discordant xenogeneic parenchymal-nonparenchymal interactions in human hepatocyte-repopulated mice. Am J Pathol 177:654–665

20. Tateno C, Takai-Kajihara K, Yamasaki C, Sato H, Yoshizato K 2000 Heterogeneity of growth potential of adult rat hepatocytes in vitro. Hepatology 31:65–74

21. Igarashi Y, Tateno C, Tanaka Y, Tachibana A, Utoh R, Kataoka M, Ohdan H, Asahara T, Yoshizato K 2008 Engraftment of human hepatocytes in the livers of rats reconstructed with bone marrow cells from an immunodeficient mouse. Xenotransplantation 15:235–245

22. Asahina K, Sato H, Yamasaki C, Kataoka M, Shiokawa M, Katayama S, Tateno C, Yoshizato K 2002 Pleiotrophin/HB-GAM as a mitogen of rat hepatocytes and its role in regeneration and development of liver. Am J Pathol 160:2191–2205

23. Gosteli-Peter MA, Winterhalter KH, Schmid C, Froesch ER, Zapf J 1994 Expression and regulation of insulin-like growth factor (IGF-I) and IGF-binding protein messenger ribonucleic acid levels in tissues and hypophysectomized rats infused with-IGF-I and growth hormone. Endocrinology 135:2558–2567

24. Thissen JP, Pucilowska JB, Underwood LE 1994 Differential reg-

ulation of insulin-like growth factor I (IGF-I) and IGF binding protein-1 messenger ribonucleic acids by amino acid availability and growth hormone in rat hepatocyte primary culture. Endocrinology 134:1570–1576

25. Benjamini Y, Hochberg Y 1995 Controlling the false discovery rate: a practical and powerful approach to multiple testing. J Roy Stat Soc Ser B 57:289–300

26. Ståhlberg N, Merino R, Hernández LH, Fernández-Pérez L, Sandelin A, Engström P, Tollet-Egnell P, Lenhard B, Flores-Morales A 2005 A Exploring hepatic hormone actions using a compilation of gene expression profiles. BMC Physiol 5:8

27. Glaser C, Heinrich J, Koletzko B 2010 Role of FADS1 and FADS2 polymorphisms in polyunsaturated fatty acid metabolism. Metabolism 59:993–999

28. Ma J, Yan R, Zu X, Cheng JM, Rao K, Liao DF, Cao D 2008 Aldo-keto reductase family 1 B10 affects fatty acid synthesis by regulating the stability of acetyl-CoA carboxylase-α in breast cancer cells. J Biol Chem 283:3418–3423

29. Ntambi JM 1992 Dietary regulation of stearoyl-CoA desaturase 1 gene expression in mouse liver. J Biol Chem 267:10925–10930

30. Menendez JA, Lupu R 2007 Fatty acid synthase and the lipogenic phenotype in cancer pathogenesis. Nat Rev Cancer 7:763–777

31. Choi CS, Savage DB, Kulkarni A, Yu XX, Liu ZX, Morino K, Kim S, Distefano A, Samuel VT, Neschen S, Zhang D, Wang A, Zhang XM, Kahn M, Cline GW, Pandey SK, Geisler JG, Bhanot S, Monia BP, Shulman GI 2007 Suppression of diacylglycerol acyltransferase-2 (DGAT2), but not DGAT1, with antisense oligonucleotides reverses diet-induced hepatic steatosis and insulin resistance. J Biol Chem 282:22678–22688

32. Baulande S, Lasnier F, Lucas M, Pairault J 2001 Adiponutrin, a transmembrane protein corresponding to a novel dietary- and obesity-linked mRNA specifically expressed in the adipose lineage. J Biol Chem 276:33336–33344

33. Huang Y, He S, Li JZ, Seo YK, Osborne TF, Cohen JC, Hobbs HH 2010 A feed-forward loop amplifies nutritional regulation of PNPLA3. Proc Natl Acad Sci USA 107:7892–7897

34. Améen C, Lindén D, Larsson BM, Mode A, Holmäng A, Oscarsson J 2004 Effects of gender and GH secretory pattern on sterol regulatory element-binding protein-1c and its target genes in rat liver. Am J Physiol Endocrinol Metab 287:E1039–E1048

35. Frick F, Lindén D, Améen C, Edén S, Mode A, Oscarsson J 2002 Interaction between growth hormone and insulin in the regulation of lipoprotein metabolism in the rat. Am J Physiol Endocrinol Metab 283:E1023–E1031

36. Shimano H, Yahagi N, Amemiya-Kudo M, Hasty AH, Osuga J, Tamura Y, Shionoiri F, Iizuka Y, Ohashi K, Harada K, Gotoda T, Ishibashi S, Yamada N 1999 Sterol regulatory element-binding protein-1 as a key transcription factor for nutritional induction of lipogeneic enzyme genes. J Biol Chem 274:35832–35839

37. Carlsson L, Nilsson I, Oscarsson J 1998 Hormonal regulation of liver fatty acid-binding protein *in vivo* and *in vitro*: effects of growth hormone and insulin. Endocrinology 139:2699–2709

38. Panici JA, Wang F, Bonkowski MS, Spong A, Bartke A, Pawlikowska L, Kwok PY, Masternak MM 2009 Is altered expression of hepatic insulin-related genes in growth hormone receptor knockout mice due to GH resistance or a difference in biological life spans? J Gerontol A Biol Sci Med Sci. 2009 64:1126–1133

39. Liu JL, Coschigano KT, Robertson K, Lipsett M, Guo Y, Kopchick JJ, Kumar U, Liu YL 2004 Disruption of growth hormone receptor gene causes diminished pancreatic islet size and increased insulin sensitivity in mice. Am J Physiol Endocrinol Metab 287:E405–E413

40. Dominici FP, Arostegui Diaz G, Bartke A, Kopchick JJ, Turyn D 2000 Compensatory alterations of insulin signal transduction in liver of growth hormone receptor knockout mice. J Endocrinol 166:579–590

41. Wauthier V, Waxman DJ 2008 Sex-specific early growth hormone response genes in rat liver. Molecular Endocrinology 22:1962–1974

42. Wauthier V, Sugathan A, Meyer RD, Dombkowski AA, Waxman DJ 2010 Division of cell and molecular biology intrinsic sex differences in the early growth hormone responsiveness of sex-specific genes in mouse liver. Mol Endocrinol 24:667–678

43. Tollet-Egnell P, Flores-Morales A, Stavréus-Evers A, Sahlin L, Norstedt G 1999 Growth hormone regulation of SOCS-2, SOCS-3, and CIS messenger ribonucleic acid expression in the rat. Endocrinology 140:3693–3704

44. Olsson B, Bohlooly-Y M, Brusehed O, Isaksson OG, Ahrén B, Olofsson SO, Oscarsson J, Törnell J 2003 Bovine growth hormonetransgenic mice have major alterations in hepatic expression of metabolic genes. Am J Physiol Endocrinol Metab 285:E504–E511

45. Hansen TK, Thiel S, Dall R, Rosenfalck AM, Trainer P, Flyvbjerg A, Jørgensen JO, Christiansen JS 2001 GH strongly affects serum concentrations of mannan-binding lectin: evidence for a new IGF-I independent immunomodulatory effect of GH. J Clin Endocrinol Metab 86:5383–5388

46. Yamamoto M, Clark JD, Pastor JV, Gurnani P, Nandi A, Kurosu H, Miyoshi M, Ogawa Y, Castrillon DH, Rosenblatt KP, Kuro-o M 2005 Regulation of oxidative stress by the anti-aging hormone klotho. J Biol Chem 280:38029–38034

47. Younossi ZM, Gorreta F, Ong JP, Schlauch K, Del Giacco L, Elariny H, Van Meter A, Younoszai A, Goodman Z, Baranova A, Christensen A, Grant G, Chandhoke V 2005 Hepatic gene expression in patients with obesity-related non-alcoholic steatohepatitis. Liver Int 25:760–771

48. Schuetz EG, Li D, Omiecinski CJ, Muller-Eberhard U, Kleinman HK, Elswick B, Guzelian PS 1988 Regulation of gene expression in adult rat hepatocytes cultured on a basement membrane matrix. J Cell Physiol 134:309–323

Regular Article

In Vitro Evaluation of Cytochrome P450 and Glucuronidation Activities in Hepatocytes Isolated from Liver-Humanized Mice

Chihiro Yamasaki[1,2], Miho Kataoka[2], Yumiko Kato[1], Masakazu Kakuni[1], Sadakazu Usuda[3],

Yoshihiro Ohzone[4], Sunao Matsuda[4], Yasuhisa Adachi[4], Shin-ichi Ninomiya[4], Toshiyuki Itamoto[5],

Toshimasa Asahara[5], Katsutoshi Yoshizato[1,6] and Chise Tateno[1,2,*]

[1]*PhoenixBio, Co., Ltd., Higashihiroshima, Japan*
[2]*Cooperative Link of Unique Science and Technology for Economy Revitalization,*
Hiroshima Prefectural Institute of Industrial Science and Technology; Higashihiroshima, Japan
[3]*ImmunoJapan Inc., Tokyo, Japan*
[4]*Sekisui Medical Inc., Tokai, Japan*
[5]*Hiroshima University, Graduate School of Biomedical Sciences, Division of Frontier Medical Science,*
Department of Surgery and Hiroshima University 21st Century COE Program for
Advanced Radiation Casualty Medicine, Programs for Biomedical Research, Hiroshima, Japan
[6]*Graduate School of Science, Hiroshima University, Higashihiroshima, Japan*

Full text of this paper is available at http://www.jstage.jst.go.jp/browse/dmpk

Summary: Cryopreserved human (h-) hepatocytes are currently regarded as the best *in vitro* model for predicting human intrinsic clearance of xenobiotics. Although fresh h-hepatocytes have greater plating efficiency on dishes and greater metabolic activities than cryopreserved cells, performing reproducible studies using fresh hepatocytes from the same donor and having an "on demand" supply of fresh hepatocytes are not possible. In this study, cryopreserved h-hepatocytes were transplanted into albumin enhancer/promoter-driven, urokinase-type plasminogen activator, transgenic/severe combined immunodeficient (uPA/SCID) mice to produce chimeric mice, the livers of which were largely replaced with h-hepatocytes. We determined whether the chimeric mouse could serve as a novel source of fresh h-hepatocytes for in vitro studies. h-Hepatocytes were isolated from chimeric mice (chimeric hepatocytes), and cytochrome P450 (P450) activities were determined. Compared with cryopreserved cells, the P450 (1A2, 2C9, 2C19, 2D6, 2E1, 3A) activities of fresh chimeric hepatocytes were similar or greater. Moreover, ketoprofen was more actively metabolized through glucuronide conjugates by fresh chimeric hepatocytes than by cryopreserved cells. We conclude that chimeric mice may be a useful tool for supplying fresh h-hepatocytes on demand that provide high and stable phase I enzyme and glucuronidation activities.

Keywords: human hepatocytes; chimeric mice; cytochrome P450; ketoprofen; UDP-glucuronosyltransferase

Introduction

"Chimeric mice" with livers repopulated with human hepatocytes (h-hepatocytes), created using urokinase-type plasminogen activator (uPA)/severe combined immunodeficient (SCID) mice,[1] were previously established and the expression of both cytochrome P450 enzymes (P450s, CYPs) and phase II enzymes in the liver of these chimeric mice, as well as *in vivo* induction of P450, were examined.[1-4]

P450 has been found to play an important role in the metabolism of xenobiotics, including drugs. Indeed, approximately 80% of oxidative metabolism is catalyzed by P450s,[5] and to predict pharmacokinetics and drug interactions precisely, investigation of the pharmacokinetics of a P450 substrate using chimeric mice would be of considerable value.

Species differences are known to exist in the metabolism of ketoprofen.[6] Ketoprofen is a propionic acid-class nonsteroidal anti-inflammatory drug with analgesic and

539

antipyretic effects. Rat and mouse P450s primarily metabolize ketoprofen to hydroxyketoprofen.[6,7] In humans, ketoprofen is primarily metabolized by UDP-glucuronosyltransferase (UGT) and is converted to ketoprofen glucuronides.[8] Recently, it was demonstrated that when chimeric mice were administered ketoprofen, glucuronide conjugates were detected in their sera and bile. However, these conjugates are minor products; ketoprofen was primarily hydrolyzed in mice, and the main metabolites were hydrolyzed ketoprofen and glucuronide-conjugated ketoprofen.[7]

The metabolism of chemical entities has been examined using animals in the laboratory, but this approach fails to address differences in drug metabolism that exist between animal species. Because of the species differences in metabolic abilities, fresh h-hepatocytes are a better model for predicting the metabolism of drugs in the human body. For technical reasons, preparing fresh h-hepatocytes ahead of time and performing reproducible studies using the same donor are not possible. Thus, cryopreserved h-hepatocytes have been used, but they are compromised on thawing, resulting in decline and alteration of their normal function. Additionally, h-hepatocytes exhibit large individual differences in P450 activities. The differences might be due to real individual differences and/or the cryopreserving and thawing conditions.

We hypothesized that these practical problems in using h-hepatocytes for in vitro drug testing could be addressed if h-hepatocytes isolated from chimeric mouse livers exhibited human-type drug metabolism capacities in vitro. In the present study, we first determined the yield, viability, and purity of isolated h-hepatocytes from chimeric mice (chimeric hepatocytes). We compared the P450 activities of fresh and cryopreserved chimeric hepatocytes and assessed glucuronide activities toward ketoprofen using fresh and cryopreserved chimeric hepatocytes and cryopreserved donor hepatocytes.

We demonstrate that the chimeric mouse liver is a useful tool that can supply fresh hepatocytes retaining high P450 and UGT activities and allowing reproducible assays using hepatocytes derived from the same donor.

Materials and Methods

Materials: Phenacetin, tolbutamide, S-mephenytoin, dextromethorphan, chlorzoxazone, testosterone, ketoprofen, and Krebs-Henseleit buffer (KHB) were purchased from Sigma-Aldrich (St. Louis, MO). Coumarin and midazolam were obtained from Wako Pure Chemical Industries (Osaka, Japan). All other chemicals and solvents were of the highest or analytical grade commercially available.

Generation of mice with humanized livers: The present study was approved by the ethics committee of PhoenixBio Co., Ltd. and the Hiroshima Prefectural In-

stitute of Industrial Science and Technology Ethics Board.

Cryopreserved h-hepatocytes from three donors (4YF, a 4-year-old Caucasian girl; 6YF, a 6-year-old African-American girl; and 2YM, a 2-year-old Caucasian boy) were purchased from BD Biosciences (San Jose, CA). Three (donor 4YF), 17 (donor 6YF), and 4 (donor 2YM) chimeric mice with humanized livers, generated by a method described previously, were used.[1] The concentration of human albumin (hAlb) in the blood of the chimeric mice and the replacement index (RI, the rate of hepatocyte replacement from mouse to human) were well correlated.[1] In the current study, we used 11–15-week-old male and female chimeric mice with approximately 11–14 mg/mL hAlb in mouse blood (RI > 70%); uPA/SCID mice were used as controls.

Isolation of hepatocytes from chimeric mouse liver, SCID mouse liver, and human liver tissue: Hepatocytes were isolated from the 4YF-, 6YF-, and 2YM-chimeric mice using a two-step collagenase perfusion method. The liver was perfused at 38°C for 10 min at 1.5 mL/min with Ca^{2+}-free and Mg^{2+}-free Hanks' balanced salt solution (CMF-HBSS) containing 200 mg/mL ethylene glycol tetraacetic acid (EGTA), 1 mg/mL glucose, 10 mM N-2-hydroxyethylpiperazine-N'-2-ethanesulfonic acid (HEPES), and 10 μg/mL gentamicin. The perfusion solution was then changed to CMF-HBSS containing 0.05% collagenase (Wako Pure Chemical Industries), 0.6 mg/mL $CaCl_2$, 10 mM HEPES, and 10 μg/mL gentamicin, and perfusion was continued for 17–23 min at 1.5 mL/min. The liver was dissected and transferred to a dish; liver cells were gently disaggregated in the dish with CMF-HBSS containing 10% bovine Alb, 10 mM HEPES, and 10 μg/mL gentamicin. The disaggregated cells were centrifuged three times (50 × g, 2 min). The pellet was suspended in medium consisting of Dulbecco's modified Eagle's medium (DMEM), 10% fetal bovine serum (FBS), 20 mM HEPES, 44 mM $NaHCO_3$, and antibiotics (100 IU/mL penicillin G and 100 μg/mL streptomycin). Cell number and viability were assessed using the trypan blue exclusion test.

Normal liver tissues were obtained from the resected liver of nine patients (51-, 53-, and 64-year-old men and a 68-year-old woman for plating efficiency; 54-, 57-, and 75-year-old men for P450 activity; and 55- and 69-year-old women for screening of monoclonal antibodies) after receiving consent prior to surgery, in accordance with the 1975 Declaration of Helsinki. Hepatocytes were isolated via two-step collagenase perfusion and low-speed centrifugation.[1] Aliquots of freshly isolated hepatocytes from four individuals, used for determining plating efficiency, were suspended at $1-2 \times 10^7$ cells/mL/vial in cryopreservation solution (Cellbanker; Juji Field, Inc., Tokyo, Japan), cryopreserved using a program freezer (Kryo-10 Series III; Planer Products Ltd., Sunbury-on-

Thames, Middlesex, UK), and kept in liquid nitrogen. To measure the plating efficiency of the hepatocytes, 4YF-chimeric hepatocytes and hepatocytes from human livers were inoculated onto 13.5-mm Celldesks (Sumitomo Bakelite, Tokyo, Japan) in 24-well plates (BD Biosciences) for 24 h, followed by fixation with ethanol and staining with hematoxylin and eosin. Adhered hepatocytes were counted under the microscope and plating efficiency was calculated by dividing number of adhered cells by the cell number inoculated in a well.

Hepatocytes were isolated from three male uPA (wt/wt)/SCID mice by collagenase perfusion methods.[9] They were used for *in vitro* glucuronidation activity studies.

Purification of h-hepatocytes from total hepatocytes of the chimeric mouse livers: A Fischer 344 rat was immunized intraperitoneally three times (once a week) with 10^7 mouse hepatocytes (m-hepatocytes) of SCID mice as an antigen, and injected with a booster of 2.5×10^7 m-hepatocytes at 3 weeks after the last immunization. Hybridomas were obtained by conventional methods and screened on immunohistochemical sections using m- and h- (from a 55-year-old woman) liver tissues. Frozen h- and m- liver sections were incubated with hybridoma supernatants and fluorescein-labeled anti-rat IgG antibodies (Alexa Fluor 594; Molecular Probes, Eugene, OR). Supernatants from 10 hybridoma clones were reacted with the plasma membrane of m-hepatocytes, but not with h-hepatocytes on the sections. The reactivity of each of the supernatants to the cell surface was determined with a fluorescence-activated cell sorter (FACS) as follows. Isolated m- and h- (69-year-old woman) hepatocytes were incubated with the supernatants and fluorescein isothiocyanate (FITC)-conjugated second antibodies (Alexa Fluor 488; Molecular Probes) and analyzed with a FACS Vantage SE (BD Biosciences) using a 100-μm nozzle. Fluorescence excited at 488 nm was measured through a 530-nm filter (FL1) with 4-decade logarithmic amplification. A hybridoma clone was selected as the clone that produced antibodies reactive to the cell surface of m-hepatocytes, but not h-hepatocytes. The antibody was purified from the culture medium of the hybridoma cells by protein G affinity column or ion exchange chromatography; the antibody was named 66Z.

Isolated h-hepatocytes from chimeric mice were contaminated with m-hepatocytes. To remove the m-hepatocytes, 6YF-hepatocytes isolated from the chimeric mice were incubated with the 66Z antibody, washed with DMEM containing 10% FBS, and incubated with Dynabeads M450-conjugated sheep anti-rat IgG (Dynal Biotech, Milwaukee, WI) in a tube for 30 min on ice. The tube was placed in Dynal MPC-1 (Dynal Biotech) for 1–2 min to remove 66Z-positive ($66Z^+$) m-hepatocytes. Enriched h-hepatocytes were collected as 66Z-negative ($66Z^-$) cells. Aliquots of chimeric hepatocytes from be-

fore and after enrichment were incubated with FITC-conjugated 66Z antibodies, and the proportion of $66Z^+$-cells in the h-hepatocytes was determined by FACS.

***In vitro* metabolic study using hepatocytes and microsomes:** For the measurement of the P450 activities of four fresh and five cryopreserved 6YF-chimeric mice, cryopreserved donor cells (6YF), and fresh h-hepatocytes from three individuals, suspended hepatocytes (6×10^4 cells) were incubated in KHB with each of eight substrates specific for seven P450 subtypes (phenacetin for CYP1A2, coumarin for CYP2A6, tolbutamide for CYP2C9, S-mephenytoin for CYP2C19, dextromethorphan for CYP2D6, chlorzoxazone for CYP2E1, and midazolam and testosterone for CYP3A) in 96-well plates (BD Biosciences) for 1 or 2 h (**Table 1**). The incubated solution was collected and an equivalent volume of methanol containing 1 μM niflumic acid (internal standard) was added. After centrifugation (10,000 rpm), the supernatant was subjected to liquid chromatography-tandem mass spectrometry (LC-MS/MS) (MDS SCIEX; Applied Biosystems, Foster City, CA). The LC system consisted of an HP 1100 system including a binary pump, an automatic sampler, and a column oven (Agilent Technologies, Waldbronn, Germany), equipped with a Symmetry Shield C18 column (Waters, Tokyo, Japan). The column temperature was 35°C. The mobile phase was 40% acetonitrile/0.1% formic acid (v/v). The flow rate was 0.3 mL/min. The LC was connected to a PE Sciex API2000 tandem mass spectrometer (Applied Biosystems), operated in positive electrospray ionization mode. The turbo gas was maintained at 550°C. Nitrogen was used as the nebulizing gas, turbo gas, and curtain gas at 65, 85, and 30 psi, respectively. Parent and/or fragment ions were filtered in the first quadrupole and dissociated in the collision cell using nitrogen as the collision gas. The analytical conditions for each substrate are shown in **Table 2**. The experiments were performed in triplicate per mouse, and the results are expressed as the average value of three mice or humans.

To assess changes in the P450 activities of fresh and cryopreserved 2YM-chimeric hepatocytes during storage at 4°C for 3 and 6 h, fresh and cryopreserved chimeric hepatocytes were prepared from two 2YM chimeric mice. The isolated hepatocytes from the chimeric mice were purified by isodensity centrifugation (27% Percoll, 7 min, 4°C) to remove dead hepatocytes. Cells (4×10^5 cells) were incubated in KHB with four different substrates specific for four P450s (phenacetin for CYP1A2, diclofenac for CYP2C9, S-mephenytoin for CYP2C19, and midazolam for CYP3A) in 24-well plates (BD Biosciences) for 2 h (**Table 1**). The incubated solution was collected and the concentration of the metabolites was measured by high-performance liquid chromatography (HPLC; Lachome Elite; Hitachi High-Technology Co., Tokyo, Japan). HPLC was performed at

Table 1. Reaction conditions for determination of CYP activities using cells and microsomes for LC-MS/MS and HPLC analysis

Enzymes measured	Enzyme activity	Substrate (concentration, mM)	Metabolite	Cells (LC-MS/MS) Incubation time (h)	Cells (HPLC) Incubation time (h)	Microsomes (LC-MS/MS) Buffer*	Microsomes (LC-MS/MS) Incubation time (min)
CYP1A2	Phenacetin O-deethylase	Phenacetin (15)	Acetaminophen	2	2	PB	20
CYP2A6	Coumarin 7-hydroxylase	Coumarin (8)	7-Hydroxycoumarin	2	—	TB	20
CYP2C9	Tolbutamide 4-hydroxylase	Tolbutamide (150)	Hydroxytolbutamide	2	—	TB	10
	Diclofenac 4'-hydroxylase	Diclofenac (100)	4-Hydroxydiclofenac	—	2	—	—
CYP2C19	S-Mephenytoin 4'-hydroxylase	S-Mephenytoin (20)	(±)-4'-Hydroxymephenytoin	2	2	PB	20
CYP2D6	Dextromethorphan O-demethylase	Dextromethorphan (8)	Dextrorphan	2	—	PB	20
CYP2E1	Chlorzoxazone 6-hydroxylase	Chlorzoxazone (100)	6-Hydroxychlorzoxazone	2	—	PB	20
CYP3A	Midazolam 1'-hydroxylase	Midazolam (10)	1'-Hydroxymidazolam	1	2	PB	10
	Testosterone 6β-hydroxylase	Testosterone (50)	6β-Hydroxytestosterone	2	—	PB	10

*TB, Tris-HCl buffer (pH 7.5); PB, potassium phosphate buffer (pH 7.4).

Table 2. Analytical parameters of LC-MS/MS for CYP1A2, 2A6, 2C9, 2C19, 2D6, 2E1, and 3A assays

Enzymes measured	Analyte	Mode	Declustering potential (eV)	Collision energy (eV)	Entrance potential (eV)	Collision cell exit potential (eV)	Ionspray voltage (V)	Analyte m/z transition
CYP1A2	Acetaminophen	Positive	40	25	7	10	5000	152.2→110.3
CYP2A6	7-Hydroxycoumarin	Positive	80	30	7	10	4200	162.8→107.2
CYP2C9	Hydroxytolbutamide	Positive	40	25	7	10	5000	286.9→171.3
CYP2C19	(±)-4'-Hydroxymephenytoin	Positive	80	25	7	10	4200	234.9→150.1
CYP2D6	Dextrorphan	Positive	120	40	7	10	4200	259.0→200.2
CYP2E1	6-Hydroxychlorzoxazone	Negative	−80	−25	−7	−10	−4200	184.1→120.0
CYP3A	6β-Hydroxytestosterone	Positive	60	25	7	10	4200	305.9→270.3
	1'-Hydroxymidazolam	Positive	100	40	7	10	5000	341.6→203.3
Ketoprofen	Ketoprofen	Positive	80	35	7	10	5000	255.5→104.9

a flow rate of 1.0 mL/min using the CAPCELL PAK C18, UG120 (4.6 × 250 mm, 5 μm; Shiseido, Tokyo, Japan) for CYP1A2 and CYP2C19, Inertsil ODS-3 (4.6 × 250 mm, 5 μm; GL Sciences Inc., Tokyo, Japan) for CYP2C9, and Xterra RP18 (4.6 × 150 mm, 5 μm; Waters) for CYP3A. Other analytical conditions are shown in **Table 3.** The measurements were performed in duplicate.

Liver microsomes were prepared from a 6YF-chimeric mouse and control uPA/SCID mice as described previously.[10] They were stored at −80°C until analysis. The protein concentration was determined using a Bradford protein assay kit (Bio-Rad, Hercules, CA), using bovine serum albumin as the standard. Microsomes from a chimeric mouse liver, pooled microsomes of six uPA/SCID mice, and pooled microsomes of 20 human

livers (BD Gentest; BD Biosciences) were incubated with the substrates at 37°C for 5 min following incubation with the reduced form of nicotinamide adenine dinucleotide phosphate (NADPH) cofactor solution (3.8 mM β-NADP$^+$, 9.7 mM glucose-6-phosphate, 9.7 mM MgCl$_2$, 1.2 U/mL glucose-6-phosphate dehydrogenase) at 37°C for 10 or 20 min (**Table 1**). The incubated solution was collected and the concentration of the metabolites was measured by LC-MS/MS. The experiments were performed in triplicate per microsome preparation, and the results are expressed as the average value.

Detection of CYP2A6 gene mutations by the Invader assay: CYP2A6 polymorphism was determined by BML, Inc. (Tokyo, Japan). Genomic DNA was isolated from thawed human hepatocytes and the DNA was used

Table 3. Analytical conditions of HPLC for CYP 1A2, 2C9, 2C19, and 3A assays

Enzymes measured	Analyte	Internal standard	Injection volume (μL)	Mobile phase			Column temperature (°C)	UV detection (nm)
				Solvent A*	Solvent B	Gradient program, %B (min)		
CYP1A2	Acetaminophen	0.1 μg Caffeine monohydrate	95	50 mM PB (pH 4.0)	Acetonitrile	Isocratic mode (A/B = 91/9)	35	245
CYP2C9	4'-Hydroxydiclofenac	0.4 μg Phenacetin	50	0.5% (v/v) AAAS	Methanol containing 0.5% (v/v) acetic acid	40 (0)→90 (30) →90 (35)→40 (36)	50	280
CYP2C19	(±)-4'-Hydroxymephenytoin	0.1 μg Phenobarbital sodium	95	50 mM PB	Acetonitrile	Isocratic mode (A/B = 80/20)	35	240
CYP3A	1'-Hydroxymidazolam	0.01 μg Phenacetin	50	10 mM PB (pH 7.4)	Acetonitrile/methanol mixture (7/5, v/v)	30 (0)→30 (5)→60 (17) →60 (25)→30 (26)	40	263

*PB, potassium phosphate buffer; AAAS, acetic acid aqueous solution.

for determining CYP2A6 polymorphism by the Invader assay.[11]

In vitro glucuronidation activity study using hepatocytes: Ketoprofen metabolism was examined using three types of hepatocytes: fresh and cryopreserved 6YF-chimeric hepatocytes, cryopreserved donor cells (6YF), and fresh uPA(wt/wt)/SCID mouse hepatocytes. Hepatocytes (4×10^5 cells) suspended in KHB were plated in 24-well, non-treated plates (BD Biosciences) and incubated at 37°C for 15 min. The cells were treated with 1 μM ketoprofen at 37°C for 3 h. The medium was harvested and aliquots of the medium were incubated at 37°C for 4 h with 0.25 M acetic acid buffer as a solvent control (A) and with 2500 units/mL β-glucuronidase (B). Equivalent 1 N KOH was added into (B) and incubated at 80°C for 3 h (C). After incubation, an equivalent of methanol containing 1 μM niflumic acid (as an internal standard) was added. After centrifugation (10,000 rpm), the supernatant was subjected to LC-MS/MS.

The relevant concentrations can then be obtained:

[Concentration of ketoprofen in (B)] − [Concentration of ketoprofen in (A)] gives [Concentration of ketoprofen-glucuronide].

[Concentration of ketoprofen in (C)] − [Concentration of ketoprofen in (B)] gives [Concentration of transferred ketoprofen-glucuronide].

The transferred ketoprofen is the acyl glucuronide positional isomer, formed by acyl migration, which may be the glucuronide form transferred from ketoprofen-glucuronide during incubation. The experiments were performed in triplicate for a given mouse, and the results are expressed as the average value of three chimeric mice for fresh chimeric hepatocytes, the average of five chimeric mice for cryopreserved hepatocytes, and the average of three uPA(wt/wt)/SCID mice for fresh control mouse hepatocytes.

Statistics: The data were analyzed using Statcel2

(OMS Publishing Inc., Tokorozawa, Japan). Results are expressed as the mean ± SD, and the significance of the difference between two groups was analyzed by Student's *t*-test when data were normally distributed, and by Welch's *t*-test otherwise. $P < 0.05$ was deemed to indicate statistical significance.

Results

Yield, viability, and plating efficiency of isolated h-hepatocytes: Hepatocytes from the 4YF-, 6YF-, and 2YM-donors were transplanted into uPA/SCID mice, and chimeric mice were obtained bearing the respective donor hepatocytes (**Table 4**). The chimeric mice (4YF, 3 mice; 6YF, 17 mice; 2YM, 4 mice) were sacrificed at 54–83 days post-transplantation (**Table 4**). On the day they were sacrificed, blood was collected for the determination of hAlb concentrations (**Table 4**). Hepatocytes were then isolated by the collagenase perfusion method. Numbers (yield) of isolated viable hepatocytes were approximately $2-3 \times 10^7$ cells/mouse (**Table 4**). The viabilities were approximately 60–70% and 50–60% for fresh and cryopreserved chimeric hepatocytes, respectively, without Percoll purification.

The plating efficiency of hepatocytes from the chimeric mice was about 66.6 ± 3.4% (mean ± SD), while those of fresh hepatocytes and cryopreserved hepatocytes from human livers were 34.0 ± 19.3% and 9.3 ± 8.3%, respectively.

Purification of h-hepatocytes isolated from chimeric mice: Chimeric hepatocyte preparations consisted of h- and m-hepatocytes. It was found that 17.3 ± 6.7% of the fresh hepatocytes from 6YF-chimeric mice were $66Z^+$ ($n = 4$; **Table 4**) by FACS analysis. The enriched chimeric hepatocytes were found to be 3.3 ± 1.0% $66Z^+$ (m-hepatocytes; $n = 4$; **Table 4**).

P450 activities of hepatocytes from the chimeric mice: The P450 activities of hepatocytes from 6YF-chi-

Chihiro YAMASAKI, *et al.*

Table 4. Hepatocytes used for the experiments

Purpose	Origin	Fresh or cryopreserved	n (sex of host animals or patients)	hAl in mouse blood (mg/ml)	Yield of hepatocytes (×10⁷ cells)	Viability (%)	Ratio of mouse hepatocytes (%)	
							Before purification	After purification
Plating efficiency	Chimeric mouse (4YF)	Fresh	3 (M: 1, F: 2)	11.5 ± 3.6	2.90 ± 2.7/mouse	63.9 ± 6.5	N.D.*4)	N.D.
	Human liver (51–68-year-old)	Fresh	4 (M: 3, F: 1)	—	0.98 ± 0.4/g liver	87.9 ± 8.2	—	—
		Cryopreserved	4 (M: 3, F: 1)	—	—	56.2 ± 7.5*5)	—	—
CYP activities	Chimeric mouse (6YF)	Fresh	4*1) (F)	11.8 ± 0.6	1.78 ± 0.9/mouse	61.8 ± 6.9	17.3 ± 6.7	3.3 ± 1.0
		Cryopreserved	5*2) (M: 2, F: 3)	12.6 ± 2.1	—	60.5 ± 10.6*5)	5.8 ± 4.7*5)	2.1 ± 1.0*5)
	Human liver (54–75-year-old)	Fresh	3 (M: 3)	—	0.43 ± 0.4/g liver	96.1 ± 2.4	—	—
	Donor cell (6YF)	Cryopreserved	1 (F)	—	—	71.1	—	—
CYP activities at different time points after perfusion or thawing	Chimeric mouse (2YM)	Fresh	2*3) (F)	11.8	3.05*5)6)/mouse	84.8*5)6)	N.D.	N.D.
		Cryopreserved	2*3) (F)	11.8	—	86.4*5)6)	N.D.	N.D.
Glucuronide activities	Chimeric mouse (6YF)	Fresh	3 (F)	13.5 ± 2.9	3.24 ± 1.0/mouse	69.8 ± 11.2	9.8 ± 2.0	—
		Cryopreserved	5 (M: 3, F: 2)	13.4 ± 2.4	—	50.7 ± 5.1*5)	12.5 ± 7.2	—
	Donor cell (6YF)	Cryopreserved	1 (F)	—	—	86.7	—	—
	uPA (wt/wt)/SCID mouse	Fresh	3	—	1.51 ± 0.3/mouse	73.2 ± 4.7	—	—

*1) Hepatocytes from one of four mice were used for CYP1A2, 2C9, and 3A (testosterone), and those from another were used for CYP2A6, 2C19, 2D6, 2E1, and 3A (midazolam). Hepatocytes from two mice were used for all tested P450s.

*2) Hepatocytes from one of five mice were used for CYP1A2, 2C9, and 3A (testosterone); those from a second mouse were used for CYP2A6, 2C19, and 2E1; those from a third mouse were used for CYP2C19, 2D6, 3A (midazolam); and those from a fourth mouse were used for tested P450s except for CYP2C19. Those from a fifth mouse were used for all tested P450s.

*3) Hepatocytes from one of two mice were used for CYP1A2 and 3A, and those from the second mouse were used for CYP2C9 and 2C19.
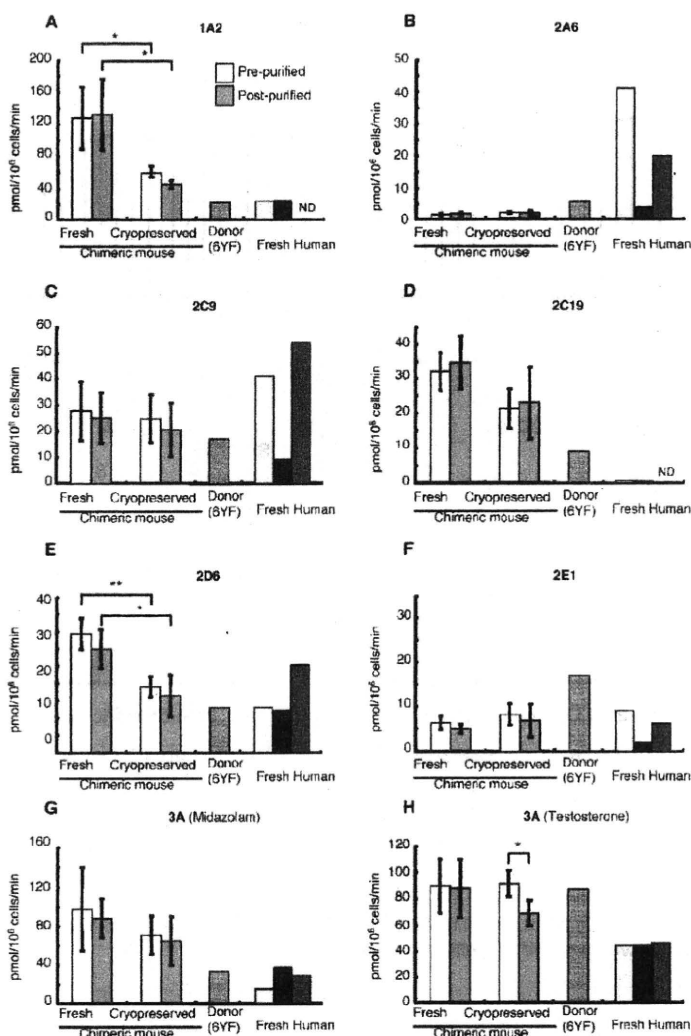
*4) Not determined.

*5) Data after thaw.

*6) Data after purification with Percoll.

meric mice were determined using eight substrates (**Table 1**). The reactions of P450 activities with all substrates shown in **Table 1** were linear with incubation time. The activities of fresh chimeric hepatocytes were compared with cryopreserved chimeric hepatocytes and cryopreserved donor cells. Three experiments were performed and the means ± SD are given in **Figure 1**. CYP1A2, 2C19, and 2D6 activities in fresh chimeric hepatocytes were approximately twice those in cryopreserved cells (**Fig. 1**). CYP2A6, 2C9, 2E1, and 3A activities in fresh chimeric hepatocytes were similar to those of cryopreserved hepatocytes (**Fig. 1**). The activities of cryopreserved donor cells (6YF) were lower than those of cryopreserved 6YF-chimeric hepatocytes in CYP1A2, 2C19, and 3A (midazolam); higher in CYP2A6 and 2E1; and similar in CYP2C9, 2D6, 3A (testosterone; **Fig. 1**). Compared with CYP2A6 activities of two of the three fresh hepatocytes, CYP2A6 activity was extremely low in the chimeric hepatocytes (**Fig. 1**). Interestingly, the Invader assay revealed that donor 6YF had the *1/*4 CYP2A6 polymorphism; livers with the *1/*4 polymor-

phism in CYP2A6 are known to show low CYP2A6 activity.[12] We concluded that the low CYP2A6 activity was due to the *1/*4 polymorphism of donor 6YF. Three kinds of fresh h-hepatocytes were also examined for P450 activity. One of the three samples did not show CYP1A2 or 2C19 activity. Large individual differences were observed among the three in CYP2A6, 2C9, and 2E1 activities. The activities of CYP1A2, 2C19, 2D6, and 3A in fresh h-hepatocytes were lower than those in fresh chimeric hepatocytes.

We determined changes in the P450 activities of fresh and cryopreserved 2YM-chimeric hepatocytes after Percoll purification during storage at 4°C after isolation and thawing, respectively. CYP1A2, 2C9, 2C19, and 3A activities did not change for up to 6 h after isolation or thawing (**Fig. 2**). CYP1A2, 2C19, and 3A activities were lower in cryopreserved chimeric hepatocytes, and CYP2C9 activity was similar compared to fresh chimeric hepatocytes at 0 h after isolation or thawing (**Fig. 2**). The results were reproducible and are similar to those in **Figure 1**.

Fig. 1. P450 activities of fresh and cryopreserved chimeric hepatocytes, cryopreserved donor hepatocytes, and fresh h-hepatocytes, determined by LC-MS/MS

Hepatocytes were isolated from 6YF-chimeric mice. Aliquots of the isolated hepatocytes were frozen with a programmed freezer. Aliquots of fresh and thawed cryopreserved chimeric hepatocytes were purified with 66Z antibodies by magnetic sorting. Cryopreserved donor hepatocytes (6YF) for the chimeric mice were thawed. Fresh h-hepatocytes were isolated from resected livers after surgery from three patients. Eight kinds of suspended hepatocytes were incubated with eight substrates specific for seven P450s (**Table 1**): (A) 1A2, (B) 2A6, (C) 2C9, (D) 2C19, (E) 2D6, (F) 2E1, (G) 3A, midazolam, and (H) 3A, testosterone. The incubated medium was analyzed for each metabolite by LC-MS/MS (**Table 2**) and the metabolic activity of each P450 is shown as pmol/10^6 cells/min. Data in fresh and cryopreserved chimeric hepatocytes are shown as means ± SD of metabolite concentrations of three different chimeric mice. $*p < 0.05$, $**p < 0.01$. ND, not detected.

Contribution of m-hepatocyte contamination in chimeric hepatocytes to P450 activity: The proportions of m-hepatocytes in the fresh chimeric hepatocytes were approximately 17% and 3% before and after purification with 66Z antibodies, respectively, as described above. To determine how the contaminating m-hepatocytes affected P450 activities, we measured P450 activities using liver microsomes from a 6YF-chimeric mouse, pooled host uPA/SCID mice, and pooled human liver microsomes. Except for CYP2D6 and 2E1,

P450 activities were similar or lower in uPA/SCID mouse liver microsomes than in human pooled microsomes (**Fig. 3**). Because the activities of CYP2D6 and 2E1 in uPA/SCID mouse liver microsomes were 50–100% higher than in pooled human microsomes (**Fig. 3**), we considered that m-hepatocytes contaminating the chimeric hepatocytes at around 17% might not significantly affect the activities of chimeric hepatocytes. We measured the P450 activity of pre- and post-purified chimeric hepatocytes (6YF) using 66Z antibodies. The purified hepato-